NEW MEXICO INSTITUTE OF MINING AND TECHNOLOGY
THE GRADUATE SCHOOL

A LEACHING MECHANISM FOR CHALCOCITE

BY

WALTER W. FISHER

A Dissertation
Submitted in partial fulfillment of the requirements
for the degree of

DOCTOR OF PHILOSOPHY IN GEOSCIENCE
(EXTRACTIVE METALLURGY)

June 1970

TABLE OF CONTENTS

LIST OF FIGURES

LIST OF TABLES

ACKNOWLEDGEMENTS

The author wishes to acknowledge Dr. Roshan B. Bhappu for his help in selecting the topic of this thesis.

The advice and criticizm of the authors advisors, Drs. Ronald J. Roman, Jacques Renault, D.K. Brandvold and Ralph M. McGehee, is gratefully acknowledged.

The New Mexico State Bureau of Mines and Mineral Resources is acknowledged for its financial support of this work.

The author wishes to express his appreciation to Mrs. Lynn Brandvold and her staff for their assistance in carrying out part of the analytic work.

And finally, the author acknowledges his wife, Vicki, for her constant moral support and for the typing of all the manuscripts of this thesis.

ABSTRACT

The oxidative dissolution of Cu_2S in oxygenated sulfuric acid solution was studied and the only reaction found to occur in the dissolution process is

$$Cu_2S + \tfrac{1}{2}O_2 + 2H^+ = CuS + Cu^{+2} + H_2O$$

where CuS is a stable reaction product.

The rate law governing the reaction is

$$R = k\,(P_{O_2})\,(H^+).$$

A reaction mechanism consistent with the experimental results is proposed. The mechanism includes both physical and chemical processes, but the rate controlling step is chemical.

INTRODUCTION

Although the dissolution of chalcocite in a variety of lixivants has been studied by many investigators (Sullivan, 1930; Warren, 1958; Stanczyk and Rampacek, 1966), none of the studies has completely defined the chemistry and mechanism of chalcocite dissolution. In particular, the mechanism of dissolution in oxygenated acid solution has not been resolved since it was first studied more than 40 years ago. The importance of chalcocite as an ore mineral in copper dumps justifies a detailed study of its dissolution in oxygenated, acid solution.

Dissolution of minerals in aqueous solution has not been studied until recently. One reason for this neglect is that these processes involve solid surface-aqueous solution reactions. This type of reaction is probably the least understood and the most difficult to approach experimentally. The reaction may be complicated by diffusion, sorption, unknown surface areas, indeterminate surface properties, lack of understanding of crystal chemistry and the unknown nature of fracture and cleavage surfaces. Some progress has been made in this area by using very pure natural minerals and synthetic mineral samples with carefully controlled stoichiometry, geometry and surface area. In addition, computer analysis allows much more extensive treatment of experimental data than has been possible in the past.

Literature Review

Sullivan (1930) studied the dissolution of chalcocite in acidified ferric sulfate and in oxygenated sulfuric acid solution. His experiments were carried out under ambient conditions at several acid and ferric ion concentrations. He found that chalcocite is oxidized by acidified ferric sulfate in two distinct stages. Although he did not identify the secondary product, he proposed that chalcocite is oxidized through the reactions given by equations (1) and (2). The overall reaction is given by equation (3).

$$Cu_2S + Fe_2(SO_4)_3 = CuSO_4 + 2FeSO_4 + CuS \qquad (1)$$

$$CuS + Fe_2(SO_4)_3 = CuSO_4 + 2FeSO_4 + S^\circ \qquad (2)$$

$$Cu_2S + 2Fe_2(SO_4)_3 = 2CuSO_4 + 4FeSO_4 + S^\circ \qquad (3)$$

Sullivan was able to identify free sulfur as the final solid reaction product. The dissolution of the intermediate product was slower than that of the original chalcocite.

Sullivan's work on chalcocite dissolution in oxygenated sulfuric acid solution only indicates that the rate of dissolution is very much slower than the rate of dissolution in ferric sulfate. He showed that in the absence of any oxidant (N_2 atmosphere) chalcocite does not react at all.

Warren (1958) studied the leaching of chalcocite in oxygenated sulfuric acid solution in an autoclave at elevated oxygen pressures and temperatures. Like Sullivan, he found that chalcocite reacts in two distinct stages. He

did not, however, postulate a reaction sequence. Warren also showed that the reaction rate increases with increases in both acidity and oxygen partial pressure. He found that the first stage of leaching has an activation energy of 6.6 kcal/mole.

Stanczyk and Rampacek (1966) investigated the leaching of various copper sulfides in an autoclave at elevated temperature and oxygen pressure. They found by microscopic examination that leached chalcocite particles were coated with covellite. They proposed that chalcocite reacts in two stages in oxygenated acid solution. Their reaction sequence is given by equations (4), (5), (6) and (7) which correspond to the overall reaction given by equation (8).

$$2Cu_2S + O_2 = 2CuS + 2CuO \quad (4)$$

$$2CuS + O_2 = 2CuO + 2SO_2 \quad (5)$$

$$4CuO + 4H_2SO_4 = 4CuSO_4 + 4H_2O \quad (6)$$

$$2SO_2 + O_2 + 2H_2O = 2H_2SO_4 \quad (7)$$

$$2Cu_2S + 2O_2 + 2H_2SO_4 = 4CuSO_4 + 4H_2O \quad (8)$$

Gerlach and Pawlek (1968) studied the leaching of several sulfide minerals in oxygenated sulfuric acid solution. They found that chalcocite leaches in two stages.

Sato (1960, 1960a) studied the dissolution of sulfide minerals from a geochemical point of view using mineral electrode potential measurements. He attribute the

dissolution of chalcocite to the two reactions given by equations (9) and (10).

$$Cu_2S = CuS + Cu^{+2} + 2e \quad (9)$$

$$CuS = Cu^{+2} + S^{o} + 2e \quad (10)$$

Kuxmann and Biallab (1969) studied the electrode potential and electrolytic dissolution of chalcocite. They attributed the dissolution of chalcocite, electrolytically or chemically, to reactions (9) and (10). They included a comprehensive literature review on the electrode potential of chalcocite.

All investigations of chalcocite dissolution have ended in postulation of a two stage reaction involving CuS as an intermediate. Most of the postulations have been made without direct proof of the reaction sequence and no identification of reaction products. Nevertheless, it appears clear that chalcocite is oxidized in two distinct steps.

Purpose and Scope

Although much work has been done on the oxidation of chalcocite by both ferric ion and oxygen, no basis has been found for the reaction sequence. Most investigators have based their work on thermodynamics and have not considered the results of chemical, kinetic, or physical studies.

The purpose of this study was to determine the reaction for the dissolution of chalcocite in oxygenated sulfuric

acid solution, establish a general rate equation for this reaction and describe a mechanism of chalcocite dissolution. This work has been based on a combination of thermodynamic, chemical, kinetic and physical studies.

THEORETICAL

The theoretical background to be presented in this section includes presentation of alternate chalcocite oxidation reactions, development of electrode potential theory, postulation of a reaction mechanism and derivation of several theoretical rate equations.

Chalcocite Dissolution Reactions

The dissolution of chalcocite in an oxygenated, aqueous environment can theoretically be accomplished by several different reactions. The reactions represented by equations (11) through (16) are all thermodynamically feasible as shown by the Gibb's free energy changes listed in Table I.

$$Cu_2S + \tfrac{1}{2}O_2 + 2H^+ = CuS + Cu^{+2} + H_2O \qquad (11)$$

$$Cu_2S + O_2 + 4H^+ = 2Cu^{+2} + S^o + 2H_2O \qquad (12)$$

$$Cu_2S + 2\tfrac{1}{2}O_2 + 2H^+ = 2Cu^{+2} + SO_4^{-2} + H_2O \qquad (13)$$

$$Cu_2S + O_2 + 2H^+ = CuO + Cu^{+2} + S^o + H_2O \qquad (14)$$

$$Cu_2S + \tfrac{1}{2}O_2 + 2H^+ = Cu^{+2} + Cu^o + S^o + H_2O \qquad (15)$$

$$CuS + \tfrac{1}{2}O_2 + 2H^+ = Cu^{+2} + S^o + H_2O \qquad (16)$$

Some of the reaction products listed in equations (11) through (16) are thermodynamically unstable. However,

Table I

The Gibb's Free Energy Change for Several Chalcocite Dissolution Reactions.

Reaction Number	Free Energy (kcal.)
11	- 34.06
12	- 65.62
13	-192.75
14	- 61.56
15	- 22.36
16	- 31.26

thermodynamic stability is usually subject to kinetic restrictions and reaction products that are unstable persist because their rate of reaction toward more stable products is very slow. For this reason, postulation of a reaction equation should be based on thermodynamics, chemical stoichiometry, and identification of products.

The investigations of Sullivan (1930), Kuxmann and Biallab (1969), and Stanczyk and Rampacek (1966) indicate that CuS is at least an intermediate product of the oxidation of chalcocite. The fact that an intermediate is observable indicates that it either reacts at a slower rate than Cu_2S or that it does not react at all. On the basis of the studies listed above, it is postulated that chalcocite is oxidized in the two steps represented by equations (11) and (16) and that the dissolution of the CuS is very slow.

$$Cu_2S + \tfrac{1}{2}O_2 + 2H^+ = CuS + Cu^{+2} + H_2O \qquad (11)$$

$$CuS + \tfrac{1}{2}O_2 + 2H^+ = Cu^{+2} + S^o + H_2O \qquad (16)$$

Electrode Potential

Comparison of experimental and theoretical electrode potentials may indicate the chemical steps that occur during a reaction. Thus, an electrode potential study may give insight into a reaction mechanism.

Theoretical

The electrode potential of the general reaction given by equation (17) is represented by equation (18) where E is

$$aA + bB = cC + dD + ne \tag{17}$$

$$E = E^{o} + \frac{2.303\ RT}{nF} \log K \tag{18}$$

the electrode potential, E^{o} is the standard potential, R is the gas constant, T is the absolute temperature, n is the number of electrons transferred in the reaction, F is Faraday's constant and K is the equilibrium constant expressed as the ratio of reactant and product activities. In this study activities are assumed to be equal to ionic concentration.

The standard potential for a reaction is given by equation (19) where ΔF_r is the Gibb's free energy change for

$$E^{o} = \frac{\Delta F_r}{nF} \tag{19}$$

the reaction and n and F have the definitions given above.

The experimental cell potential is related to the reaction potential, E, by equation (20) where E_c and E_r are

$$E = E_c - E_r \tag{20}$$

respectively the cell potential and the reference electrode potential. A saturated, calomel electrode was used as a reference for all measurements. The potential of the calomel electrode in volts as a function of temperature is given by equation (21) where T is temperature in ^{o}C.

$$E_r = 0.244 - 0.00066\ (T - 25.0) \tag{21}$$

Comparison of Potentials

When a reaction occurs in several distinct steps, it may be possible to measure the potential of at least one step as the reaction progresses. The electrode potential of hypothetical reactions can be calculated from thermodynamic data. When the experimental potential is compared to each of the hypothetical potentials, close agreement between the experimental potential and any one of the hypothetical potentials indicates which reaction accompanies the step. Table II lists the electrode reactions corresponding to equations (11) through (16) along with the electrode potentials corresponding to each reaction.

Literature Review

Sato (1960a) and Kuxmann and Biallab (1969) determined the electrode potential of chalcocite. They attributed this potential to reaction (9). Table II gives a standard

$$Cu_2S = CuS + Cu^{+2} + 2e \qquad (9)$$

potential of 0.530 V for this reaction. Both investigators suggested that variations in experimental electrode potentials are due to the stoichiometry of chalcocite. Kuxmann and Biallab (1969) reported that a chalcocite electrode containing 78.0% copper produced a potential 7 mV more negative than an electrode containing 79.3% copper. Sato (1960a) suggested that the reaction responsible for the potential of chalcocite is that given by equation (22). Since no thermodynamic data

Table II

Chalcocite Electrode Reactions and Their Standard Electrode Potentials.

Reaction	E^o (volts)
$Cu_2S = CuS + Cu^{+2} + 2e$	0.530
$Cu_2S = 2Cu^{+2} + S^o + 4e$	0.560
$Cu_2S + 2O_2 = 2Cu^{+2} + SO_4^{-2} + 2e$	-2.908
$Cu_2S + \frac{1}{2}O_2 = CuO + Cu^{+2} + S^o + 2e$	0.124
$Cu_2S = Cu^{+2} + Cu^o + S^o + 2e$	0.783
$CuS = Cu^{+2} + S^o + 2e$	0.590

$$5Cu_2S = Cu_9S_5 + Cu^{+2} + 2e \qquad (22)$$

is available for digenite, the theoretical electrode potential for reaction (22) cannot be calculated.

Summary

The experimental electrode potential of chalcocite indicates that the first step in the oxidation reaction is given by equation (9). This is in agreement with the first reaction step postulated in the previous section.

A Reaction Mechanism

A mechanism for the oxidation and dissolution of chalcocite in any oxygenated, aqueous solution must account for both the reduction of oxygen and the oxidation of the mineral. Since the dissolution involves an aqueous solution-solid surface reaction, sorption and solid state transformations must also be considered as part of the dissolution process.

The Overall Reaction

The chemical study of Sullivan (1930), the electrochemical investigations of Kuxmann and Biallab (1969) and Sato (1960a) and the microscopic study of Stanczyk and Rampacek (1966) suggest that the dissolution of chalcocite occurs in the two steps given by equations (11) and (16).

$$Cu_2S + \tfrac{1}{2}O_2 + 2H^+ = CuS + Cu^{+2} + H_2O \qquad (11)$$

$$CuS + \tfrac{1}{2}O_2 + 2H^+ = Cu^{+2} + S^o + H_2O \qquad (16)$$

Since CuS or a CuS like compound is observable, the rate of dissolution of the intermediate, CuS, must be slower than the rate of dissolution of Cu_2S. In fact, it may be slow enough to be considered negligble. It is postulated that the only reaction of importance is given by equation (11) and that dissolution stops at the formation of CuS.

The Mechanism of Oxygen Reduction

Latimer (1952) and Huffman and Davidson (1956) suggested that oxygen is reduced through the reaction sequence given by equations (23), (24), (25) and (26) where Fe^{+2} ion is the electron donar. The overall reaction is given by equation (27).

$$Fe^{+2} + O_2 + H^+ = Fe^{+3} + HO_2 \qquad (23)$$

$$Fe^{+2} + HO_2 + H^+ = Fe^{+3} + H_2O_2 \qquad (24)$$

$$Fe^{+2} + H_2O_2 + H^+ = Fe^{+3} + OH + H_2O \qquad (25)$$

$$Fe^{+2} + OH + H^+ = Fe^{+3} + H_2O \qquad (26)$$

$$4Fe^{+2} + O_2 + 4H^+ = 4Fe^{+3} + 2H_2O \qquad (27)$$

It seems reasonable to assume that the reduction sequence of oxygen will be the same for both the oxidation of chalcocite and the oxidation of ferrous ion. Therefore, the oxygen reduction sequence will be included in the chalcocite oxidation mechanism.

The Chalcocite Oxidation Mechanism

Using equation (11), sorption of oxygen on the mineral surface, the oxygen reduction reaction sequence, and solid state reactions, the reaction sequence given by equations (28) through (39) is proposed for the dissolution of chalcocite.

The reaction mechanism implies that Cu^{+1} atoms diffuse from the interior of the Cu_2S particle creating the physical situation shown in Figure 1. As the Cu^{+1} atoms diffuse out of the Cu_2S lattice and are oxidized to Cu^{+2}, a non-stoichiometric chalcocite of the form $Cu_{2-x}S$ is created. The factor x goes from 1 at the mineral surface to 0 at the unreacted Cu_2S boundary. This physical picture of the dissolution process is proposed on the basis of the existence of CuS as a stable reaction product.

Dutrizac, MacDonald and Ingraham (1970) showed that when bornite is leached in acidified ferric sulfate solution, a non-reactive, bornite layer of the form $Cu_{5-x}FeS_4$ forms. Their electron microprobe examination of the edge of a leached bornite disk produced a picture similar to Figure 1 with CuS replaced by $Cu_{5-x}FeS_4$. They found a value of about 1.2 for x.

The mechanism represented by equations (28) through (39) is proposed without indicating which reaction might be rate controlling. The rate laws that result from assuming that different reactions control the rate will be derived in the following discussion.

$$Cu_2S\} = Cu_{2-x}S\}Cu^{+1} \quad (28)$$

$$Cu_{2-x}S\}Cu^{+1} + O_2\ (aq) = Cu_{2-x}S\}Cu^{+1}\text{--}O_2 \quad (29)$$

$$Cu_{2-x}S\}Cu^{+1}\text{--}O_2 + H^+ = Cu_{2-x}S\}Cu^{+2}\text{--}HO_2 \quad (30)$$

$$Cu_2S\ \ Cu_{2-x}S\}Cu^{+2}\text{--}HO_2 = Cu_2S\ \ CuS\}Cu^{+1}\text{--}HO_2 + Cu^{+2} \quad (31)$$

$$Cu_2S\ \ CuS\}Cu^{+1}\text{--}HO_2 + H^+ = Cu_2S\ \ CuS\}Cu^{+2}\text{--}H_2O_2 \quad (32)$$

$$Cu_2S\ \ CuS\}Cu^{+2}\text{--}H_2O_2 = Cu_{2-x}S\ \ CuS\}Cu^{+1}\text{--}H_2O_2 + Cu^{+2} \quad (33)$$

$$Cu_{2-x}S\ \ CuS\}Cu^{+1}\text{--}H_2O_2 + H^+ = Cu_{2-x}S\ \ CuS\}Cu^{+2}\text{--}OH + H_2O \quad (34)$$

$$Cu_2S\ \ Cu_{2-x}S\ \ CuS\}Cu^{+2}\text{--}OH = Cu_2S\ \ CuS\ \ CuS\}Cu^{+1}\text{--}OH + Cu^{+2} \quad (35)$$

$$Cu_2S\ \ CuS\ \ CuS\}Cu^{+1}\text{--}OH + H^+ = Cu_2S\ \ CuS\ \ CuS\}Cu^{+2} + H_2O \quad (36)$$

$$Cu_2S\ \ CuS\ \ CuS\}Cu^{+2} = Cu_{2-x}S\ \ CuS\ \ CuS\}Cu^{+1} + Cu^{+2} \quad (37)$$

$$Cu_{2-x}S\ \ CuS\ \ CuS\}Cu^{+1} + O_2\ (aq) = Cu_{2-x}S\ \ CuS\ \ CuS\}Cu^{+1}\text{--}O_2 \quad (38)$$

$$CuS\ \ CuS\ \ CuS\ \ CuS\}Cu^{+2} = \ldots\ CuS\ \ CuS\ \ CuS\} + Cu^{+2} \quad (39)$$

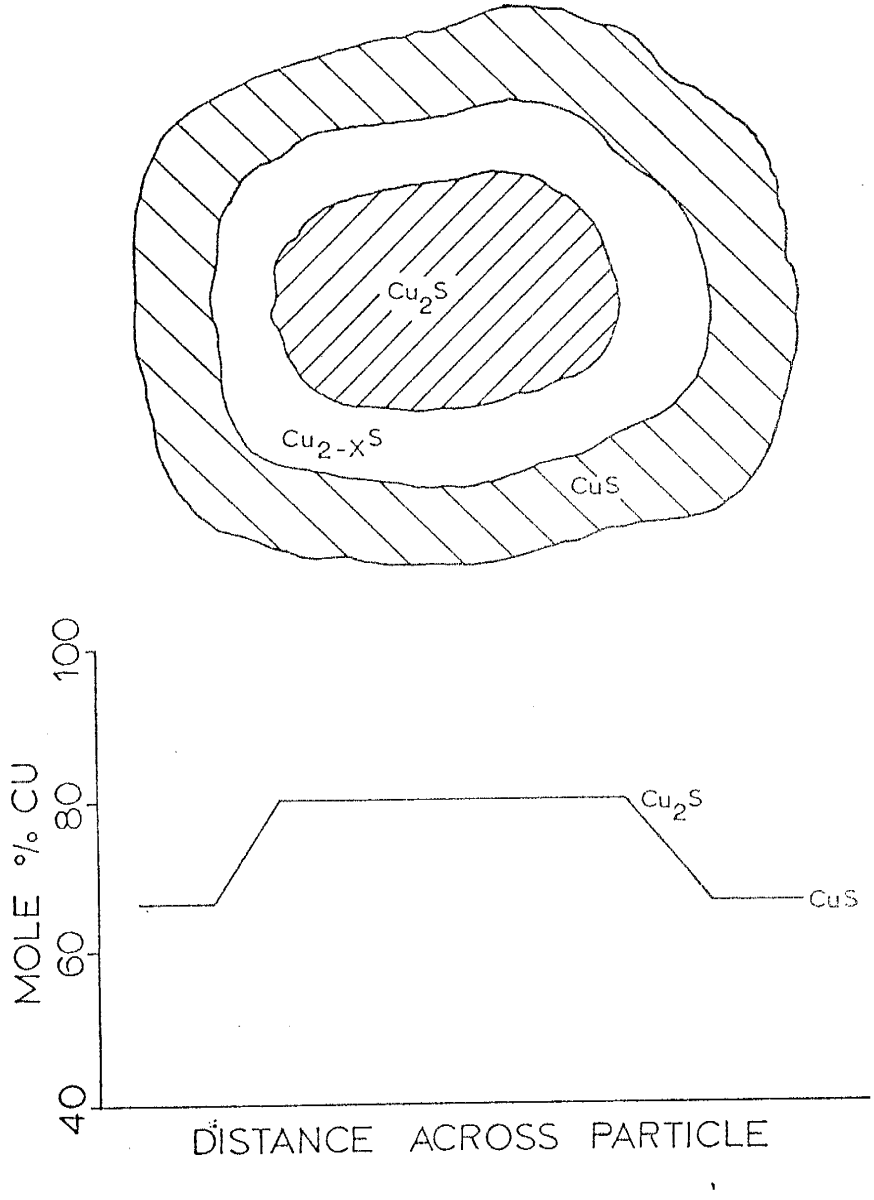

Figure 1. The Stoichiometry of a Partially Leached Chalcocite Particle.

Summary

The overall chalcocite dissolution reaction is postulated to be that given by equation (11). The proposed

$$Cu_2S + \tfrac{1}{2}O_2 + 2H^+ = CuS + Cu^{+2} + H_2O \qquad (11)$$

mechanism for the dissolution of chalcocite is represented by the reaction sequence of equations (28) through (39).

Theoretical Rate Equations

A reaction mechanism is not complete until the relative reaction velocities for each reaction in the sequence is established and a rate law consistent with experimental data has been derived from the mechanism. A reaction mechanism is made up of elementary reactions so that the stoichiometric coefficients of the reactants are the same as the order of the reaction with respect to each reactant. A theoretical rate equation can be derived from these elementary reactions by assigning relative reaction velocities to each step in the mechanism sequence.

Rate Control by Oxygen Dissolution

The first reaction in the chalcocite oxidation is actually the dissolution of O_2 gas in the solution which is represented by equation (40). If this process is rate

$$O_2\ (g) = O_{2(aq)} \qquad (40)$$

controlling, a rate law of the form given by equation (41)

$$R = k_{40} (O_2) \tag{41}$$

should result. The dissolution of O_2 in the solution does not involve the mineral, and therefore, the surface area of the mineral should not effect the rate of reaction.

Rate Control by Sorption of Oxygen

If equation (28) is assumed to establish a rapid equilibrium and equation (29) is assumed to control the

$$Cu_2S| \overset{\text{fast}}{\rightleftharpoons} Cu_{2-x}S|Cu^{+1} \tag{28}$$

$$Cu_{2-x}S|Cu^{+1} + O_{2(aq)} \overset{\text{slow}}{\rightleftharpoons} Cu_{2-x}S|Cu^{+1}\text{--}O_2 \tag{29}$$

reaction rate, then the rate law is given by equation (43)

$$R = k_{29} (Cu_{2-x}S|Cu^{+1}) (O_2) \tag{43}$$

Equation (43) is the equilibrium relation for reaction (28). Combination of equations (42) and (43) yields equation (44)

$$K_{28} = \frac{k_{28}}{k_{-28}} = \frac{(Cu_{2-x}S|Cu^{+1})}{(Cu_2S|)} \tag{43}$$

$$R = \frac{k_{28}\, k_{29}}{k_{-28}} (O_2) \tag{44}$$

as the rate law. The surface activity is assumed to be one. Positive subscripts on k indicate forward rate constants and negative subscripts indicate backward rate constants.

Since the reaction involves the mineral, the reaction rate should be a function of surface area.

Rate Control by Reduction of Oxygen

If equations (28) and (29) establish rapid equilibria and equation (30) is rate controlling, the rate law is given

$$Cu_2S| \overset{\text{fast}}{\rightleftharpoons} Cu_{2-x}S|Cu^{+1} \qquad (28)$$

$$Cu_{2-x}S|Cu^{+1} + O_{2(aq)} \overset{\text{fast}}{\rightleftharpoons} Cu_{2-x}S|Cu^{+1}\text{--}O_2 \qquad (29)$$

$$Cu_{2-x}S|Cu^{+1}\text{--}O_2 + H^+ \overset{\text{slow}}{\longrightarrow} Cu_{2-x}S|Cu^{+2}\text{--}HO_2 \qquad (30)$$

by equation (45). The equilibrium relations for reactions

$$R = k_{30}\ (H^+)\ (Cu_{2-x}S|Cu^{+1}\text{--}O_2) \qquad (45)$$

(28) and (29) are given by equations (43) and (46).

$$K_{29} = \frac{k_{29}}{k_{-29}} = \frac{(Cu_{2-x}S|Cu^{+1}\text{--}O_2)}{(O_2)\ (Cu_{2-x}S|Cu^{+1})} \qquad (46)$$

Combination of equations (43), (45) and (46) yield the rate law represented as equation (47) where the surface activity

$$R = \frac{k_{28}\ k_{29}\ k_{30}}{k_{-28}\ k_{-29}}\ (O_2)\ (H^+) \qquad (47)$$

is assumed to be one. The reaction involves the mineral and the rate should be a function of surface area.

Summary

Chemical and electrochemical investigations indicate that chalcocite is oxidized in two distinct steps and that the intermediate, CuS, may be a stable product. Therefore, it is postulated that dissolution only occurs by the reaction represented by equation (11). The work of Huffman and Davidson (1956) indicates that oxygen is reduced through the series of species, O_2 - HO_2 - H_2O_2 - OH - H_2O. A reaction mechanism based on equation (11), sorption of oxygen on the mineral surface, step-wise reduction of oxygen and solid state transformations is postulated and is represented by equations (28) through (39). Three rate laws derived from this reaction sequence are presented and will be compared to the experimentally determined rate law for chalcocite dissolution.

EXPERIMENTAL

The objectives of this study were to determine the dissolution reaction for chalcocite, establish a general rate equation for this reaction and present a reaction mechanism for the dissolution process. These objectives were accomplished in three basic studies which will be described in the following discussion.

The Mineral Sample

The samples of chalcocite used in this study were obtained from the New Cornelia Mine, Ajo, Arizona through the Southwest Scientific Company. The samples were massive pieces of chalcocite bounded on one or more sides by quartz and contained some quartz inclusions.

Physical Description

A slab of chalcocite was prepared by cutting with a diamond saw. One surface of the slab was polished and etched to bring out the grain structure. The etching solution was an aqueous solution containing 1 M $FeCl_3$ and 0.5 M HCl. The grains of chalcocite were about 5 to 8 millimeters across their maximum dimension, had irregular shapes and were interlocked to a great extent. The mineral grains were preferentially elongated so that on the average the length of the grains was 1.25 to 1.50 times the width.

The chalcocite surface showed an occasional quartz inclusion.

Microscopic examination of -48+65 mesh chalcocite that was prepared for leaching showed that the material was primarily chalcocite with 5 to 10 percent quartz (by volume) and an occasional grain of pyrite.

Identification and Analysis

An x-ray diffraction examination of a -200 mesh sample of chalcocite was performed in order to identify the minerals present. The sample was found to be a mixture of chalcocite and quartz. The experimental x-ray data is given in Appendix A, Table XII.

A sample of the mineral was submitted to examination by an emmision spectrograph to determine the impurities present. Table III lists the elements present as major, minor and trace. The major elements present are copper, silicon and iron.

On the basis of the emmision spectrograph report, a chemical analysis of the chalcocite was carried out to determine the amount of copper, iron, sulfur and quartz present. The sample was found to contain 71.48% copper, 0.55% iron, 20.03% sulfur and 7.94% quartz. Copper and iron were determined as aqueous ions, quartz as the weight of insoluble material and sulfur by weight difference.

Table III

Emmision Spectrograph Report on Chalcocite from the New Cornelia Mine, Ajo, Arizona.

Major	Minor	Trace
Si	Al	Mg
Fe	Ca	Mn
Cu	Ag	As
		W
		Co
		Mo

Preparation of Samples for Leaching

The chalcocite was prepared for leaching in the following manner. The massive pieces of mineral were broken with a hammer. The resultant pieces were about one inch in their maximum dimension. These small pieces were separated so that most of the quartz was rejected. The small pieces of chalcocite were broken and crushed with an agate mortar and pestle. The crushed material was sized with a series of Tyler screens to yield the size fractions -48+65, -65+100, +100-150, -150+200 and -200 mesh. The sized chalcocite was stored in stoppered glass bottles.

Reagents and Solutions

All of the reagents used in this study were analytic grade chemicals supplied by the J.T. Baker Chemical Compa

Most of this study was carried out with solutions containing specific concentrations of various ions at a constant ionic strength of 0.2 M. The reagents used to prepare leach solutions were added as either stable salts or standardized stock solutions.

Solutions of 1 N H_2SO_4, $HClO_4$, HNO_3, HCl and HBr were prepared by diluting the concentrated acid with distilled water, and then, standardizing the acid against a standard NaOH solution. Stock solutions of Na_2SO_4, $NaClO_4$ and $NaNO_3$ were prepared by neutralizing the acid with standard NaOH solution and diluting the neutralized mixture to a known volume. Solutions of $Cu(ClO_4)_2$, $Cu(NO_3)_2$ and $CuBr_2$ were

prepared by dissolving the proper weight of CuO in $HClO_4$, HNO_3 or HBr respectively. The resulting solutions were diluted to a known volume and analyzed for Cu^{+2} and H^+ ions. All other reagents used in preparing leach solutions were added as the salts $CuSO_4 \cdot 5H_2O$, $CuCl_2 \cdot 2H_2O$, NaCl or NaBr.

Leach solutions were prepared by combining predetermined quantities of salts and stock solutions and diluting the mixture to the appropriate volume. Thus, each leach solution was made up volumetrically so that it was not necessary to determine the concentration of each species in the initial leach solution.

The analytic procedures used in this study are given in Appendix C.

The Leaching System

Reaction Vessel

The reaction vessel used for this study was a 2.5 liter lucite chamber with an internal, overhead, magnetic stirring device. It was designed to be an ambient condition autoclave. The reaction vessel is shown schematically in Figure 2.

The vessel was designed to contain platinum, glass, reference and mineral electrodes. These electrodes were placed in the system through rubber stoppers. They allowed the measurement of pH, Eh and mineral electrode potential.

Agitation was accomplished by a three bladed, glass impellor connected to the magnetic stirring device.

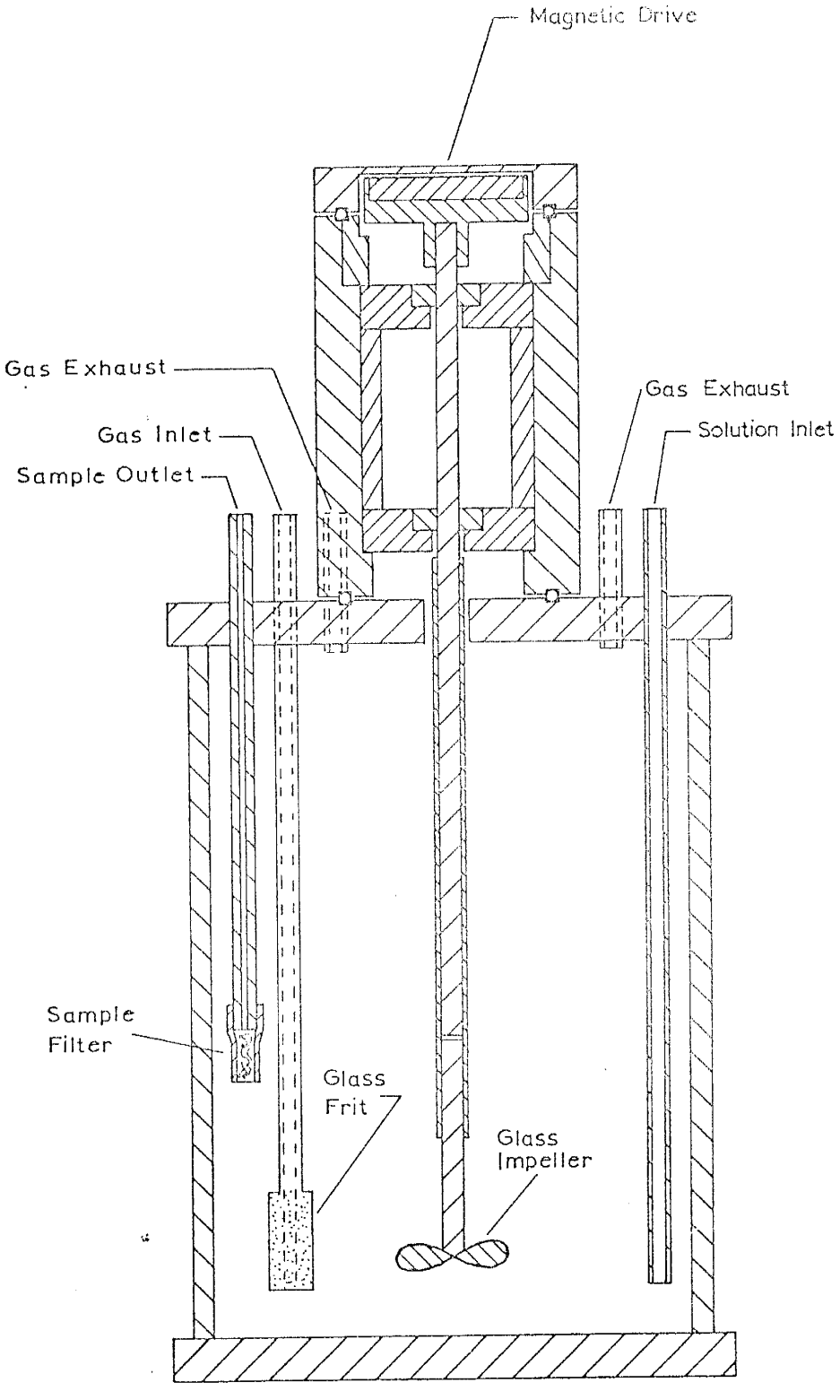

Figure 2. A Cross-Section of the 2.5 Liter Lucite Reaction Vessel.

The vessel was equipped with a sample outlet, four inlet-outlets for gases and solutions and a thermometer. The sampling outlet was fitted with a glass wool filter to prevent uptake of mineral particles. It was constructed of 0.5 millimeter capillary tubing to reduce the volume of solution trapped between samples. The main gas inlet was a glass frit diffuser which was used to insure good gas-solution contact.

The Leaching System

Figure 3 is a diagramatic representation of the leaching system. The reaction vessel and a solution storage bottle were submerged in a constant temperature bath. The bath temperature was kept at constant temperature by a Precision Scientific Company Porta Temp Controller. This unit stirs the bath in addition to controlling the temperature with an accuracy of $\pm 0.1^{\circ}C$.

The flow of gases and solutions was controlled by the valves and piping shown in Figure 3. Samples were removed from the system through a 10 ml. pipet.

The system may contain other supporting equipment not shown such as a pH meter, barometer, potentiometer, switching circuit and timer.

The versatility of this experimental setup allowed several types of experiments to be carried out in the same apparatus.

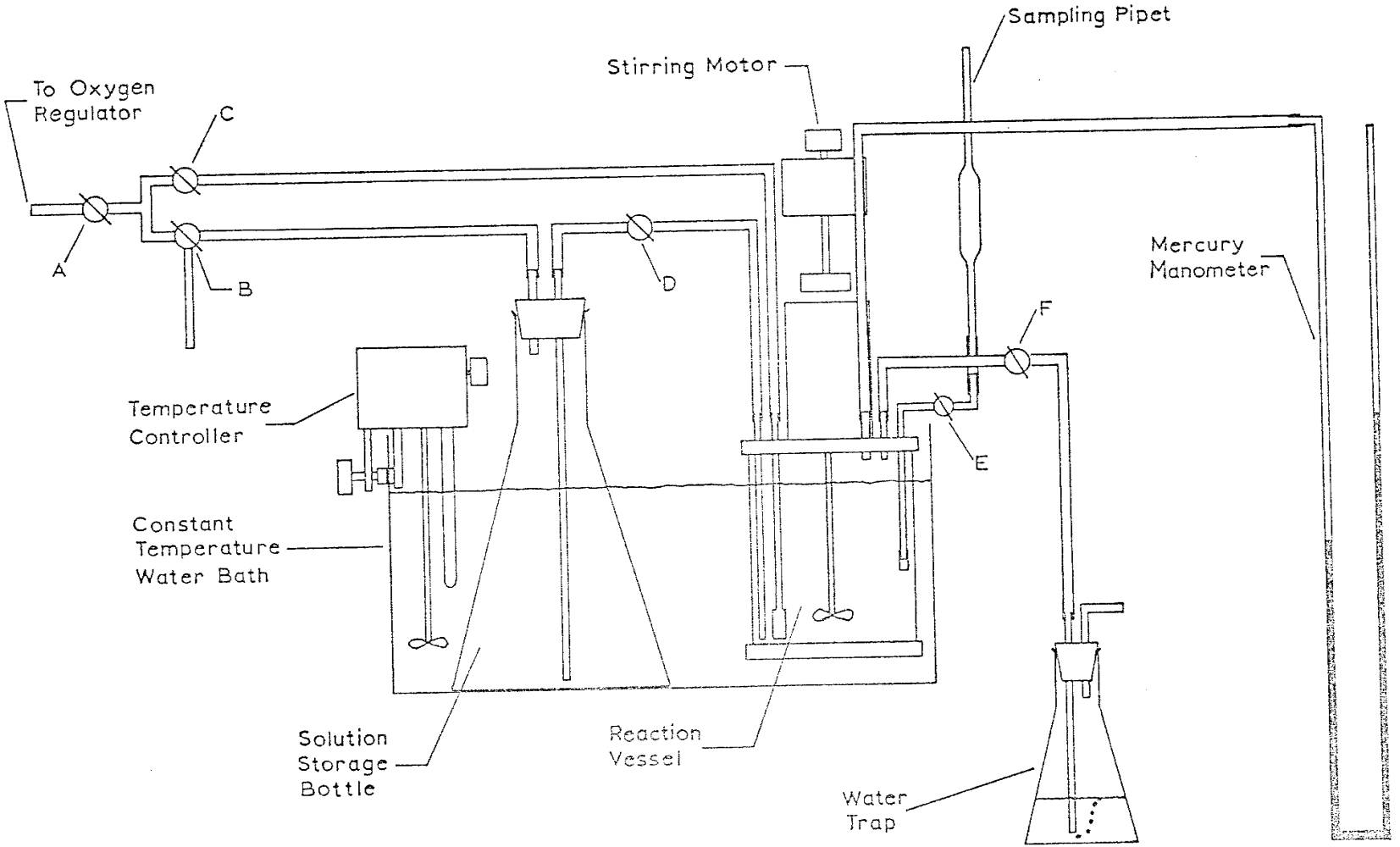

Figure 3. Schematic Representation of the Leaching System.

Mineral Electrodes

The nature of the mineral electrode is shown in Figure 4. A lucite rod 1.25 inches in diameter was machined as indicated in the diagram. A piece of chalcocite 1.9 cm on a side and about 0.5 cm thick was sealed into the lucite with Scotch Brand Epoxy manufactured by the 3M Company. The surface of the electrode was ground flat and polished. An insulated copper wire was connected to the back of the electrode with 3021 E-Solder Silver Epoxy manufactured by Epoxy Products Inc. A ¼ inch O.D. lucite tube was passed over the insulated wire and cemented into the back of the lucite holder with methylene chloride.

Experimental Procedures

Three types of experiments were performed during this study. These included determination of the electrode potential of chalcocite, the reaction stoichiometry and rate of oxygen consumption and the rate of copper dissolution.

Determination of Electrode Potential

The purpose of this part of the study was to determine the electrode potential of the reacting chalcocite surface in an aqueous solution. The concentration of all ionic species was controlled precisely. The potential measuring system consisted of the chalcocite electrode and a saturated calomel reference electrode connected to a high sensitivity

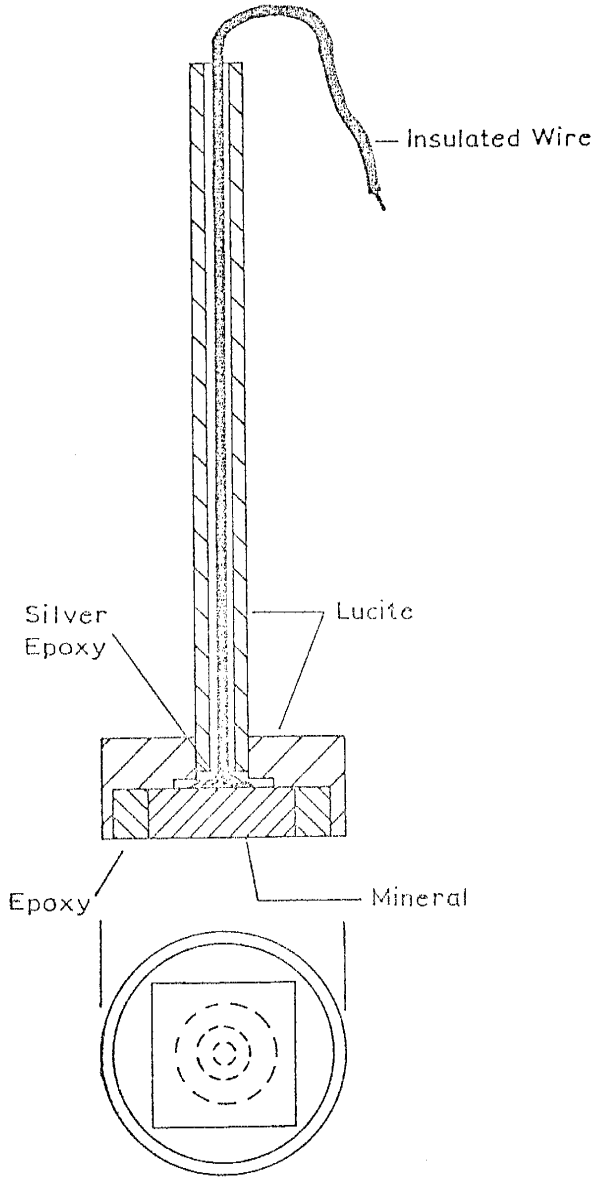

Figure 4. Details of a Mineral Electrode.

Leeds and Northrup No. 7552 Potentiometer. The emf was measured over an extended period of time to determine the equilibrium value of the rest potential.

Determination of Stoichiometry and Oxygen Consumption Rate

These experiments were designed to determine the reaction stoichiometry and the rate of oxygen consumption. The reaction stoichiometry was determined by finding the change in the concentration of hydrogen ion, cupric ion and dissolved oxygen during an experiment. Hydrogen and cupric ion concentrations were found analytically by the methods described in Appendix C. The quantity of oxygen consumed was determined from the total pressure change, system gas volume and experimental temperature using the ideal gas law. The details of this calculation are given in Appendix B.

The rate of oxygen consumption was determined by following the change in system pressure as a function of time. The pressure was measured with a water manometer. The details of the measurement, correction and conversion of the pressure are given in Appendix B.

Determination of Chalcocite Dissolution Rate

The purpose of this part of the study was to determine the effect of different variables on the rate of copper dissolution from chalcocite. The variables studied include system reproducibility, stirring rate, surface area, oxygen partial pressure, cupric ion concentration, hydrogen ion concentration, temperature, sulfate ion concentration, and

type of anion. The effect of each variable was determined by holding all other variables constant while changing the one of interest. The rate of the reaction was followed by finding the change in cupric ion concentration as a function of time. This was accomplished by taking samples of the leach solution at specified times during the course of the experiment.

Experimental Procedures

The experimental procedures for each of the three types of experiments are nearly the same. Variations occur only in the last few steps. Therefore, the initial part of the procedure which is common to all experiments will be discussed first. The variations used will be listed separately. Figure 3 is the system being described.

The initial procedure is given below.

1. The leach solution was prepared, analyzed for cupric and hydrogen ion concentration and placed in the solution storage bottle.
2. The electrodes or crushed chalcocite were placed in the reaction vessel and the vessel was sealed and placed in the water bath.
3. The necessary connections were made between the gas manifold, solution storage bottle, reaction vessel and manometer. All valves in the system were closed.

4. The constant temperature bath was brought up to and stablized at the desired temperature.
5. The reaction vessel and leach solution were purged with oxygen gas by opening valves A, C and D and opening the three-way valve B to the atmosphere. The purge was performed for a minimum of 15 minutes. After the system was purged, all valves were again closed.
6. The leaching experiment was started by transferring the leach solution from the storage bottle to the reaction vessel. Transfer was accomplished by opening valves A, B, D and F. When about 2.5 liters of solution was transferred into the reaction vessel, valves B and D were closed. The volume was indicated by marks on the reaction vessel.
7. Agitation was started by turning on the stirring motor.

At this point the different types of experiments require slightly different procedures. The procedure for the stoichiometry and oxygen consumption rate experiments is given below.

8. Valve F was closed and valve C was opened in order to pressurize the system. When the desired pressure was reached, all of the valves were closed.

9. The progress of the experiment was followed by monitoring the system pressure with a water manometer in place of the mercury manometer. The barometric pressure was also monitored.
10. At the termination of the experiment, solution samples were analyzed for cupric and hydrogen ion concentrations.
11. The vessel was filled with water to determine the original leach solution volume.

The electrode potential and copper dissolution experiments are similar and will be described together. The procedure for these experiments is given below.

8'. Value C was opened and oxygen gas was allowed to bubble through the solution in the reaction vessel. The quantity of gas passing through the system was indicated by the bubbles passing through the water trap. The system pressure was controlled by changing the oxygen regulator pressure while holding the gas flow constant by adjusting valves C and F. In experiments carried out below atmospheric pressure a vacuum was placed on the water trap and gas was allowed to flow through valve C to raise the system pressure to the desired value.

9'. When electrode potential was being determined, the change in potential was monitored with a potentiometer. When rate of copper dissolution was being determined, 10 ml solution samples were taken at specified times by opening valve E and applying a suction to the top of the pipet. After the pipet was filled, it was removed and the sample was diluted for analysis by atomic absorption. The pipet was washed, dried and replaced.

10'. The system pressure and barometric pressure were observed and recorded with each solution sample or potential reading.

11'. The vessel was filled with water to determine the original leach solution volume.

The procedures given above were used for all experiments unless indicated otherwise.

RESULTS AND DISCUSSION

The purpose of this study was to 1) determine the reaction by which chalcocite is oxidized and dissolved, 2) find a general rate equation for the dissolution of chalcocite, 3) establish the reaction sequence and 4) propose a physico-chemical reaction mechanism for chalcocite oxidation and dissolution.

The results, interpretation and discussion of the results are presented in the following sections.

Electrode Potential of Chalcocite

The purpose of this portion of the study was to determine the electrode potential of a reacting chalcocite surface.

The experimental conditions of this determination are listed in Table IV. The equilibrium cell potential was 0.13177 volt. This value was first reached after 88.3 hours elapsed time. The potential remained constant until the experiment was terminated at 304.4 hours. The standard potential of the experimental cell was found to be 0.462 volt by utilizing equations (18), (20) and (21).

Other investigators have studied the electrode potential of chalcocite. Table V is a tabulation of their results along with the result of this study. Obviously, the electrode potential of chalcocite is not a

Table IV

Experimental Conditions for the Determination of the Electrode Potential of Chalcocite.

Variable	Value
T	31.6°C
O_2	0.811 atm.
(H^+)	0.09971 M
(Cu^{+2})	0.00101 M
(Na^+)	0.04600 M
(SO_4^{-2})	0.05087 M
(ClO_4^-)	0.04600 M
I	0.1996 M

Table V

Experimental Standard Electrode Potentials for Chalcocite.

Cu_2S Source	E^o (volts)	Source of Information
Theoretical	0.530	Latimer (1952)
Natural	0.462	This study
Natural	0.505	Sato, 1960a
Synthetic	0.486	Kuxmann, 1969
Synthetic	0.470	Kuxmann, 1969
Synthetic	0.490	Kuxmann, 1969

reproducible phenomenon. Comparison of the E° values of Table V with those of Table II indicates that the experimental potentials fall closest to 0.530 volt. The reaction that corresponds to this potential is given by equation (9). All of the sources cited in Table V attribute the experimental potential to this reaction.

$$Cu_2S = CuS + Cu^{+2} + 2e \qquad (9)$$

Summary

The experimental electrode potential for a reacting chalcocite electrode was found to be 0.462 V. Other investigators have found similar values and have attributed the potential to reaction (9). On the basis of the experimental potential found in this study and the work of other investigators, the reaction producing the chalcocite electrode potential is assumed to be reaction (9).

Natural Solubility of Chalcocite

The purpose of this study was to show that chalcocite must be oxidized for appreciable dissolution of the mineral to take place. These experiments followed the procedure used for oxygen consumption experiments except that nitrogen was used in place of oxygen to produce a non-oxidizing atmosphere. All vessels and solutions were purged with N_2 gas before each experiment.

Two experiments were performed in 0.1 N H_2SO_4 solution. No other dissolved or ionic species were present except

dissolved nitrogen. The first experiment was performed on 50.0 g of -48+65 mesh chalcocite that was crushed and sized in the atmosphere. The second experiment was carried out on 23.7 g of -48+65 mesh chalcocite that was crushed and sized under an atmosphere of dry nitrogen gas. Both samples were leached under normal experimental conditions for 20 hours. After the amount of copper dissolved has been normalized to a sample weight of 25.0 g and a solution volume of 2.5 liters, the concentration of dissolved copper is 21.3 ppm and 20.4 ppm respectively. This amounts to 0.0021 grams of copper per gram of Cu_2S. Therefore, the chalcocite used in this study has a natural solubility that may be significant. The fact that the two results are almost identical indicates that crushing in the presence of oxygen has nothing to do with the solubility, and therefore, the solubility is not necessarily due to surface oxidation.

The solubility product for chalcocite listed in the Handbook of Physics and Chemistry (1960) is 2.0×10^{-47} at 18° to 20° C. This limited solubility is certainly exceeded by a concentration value of 20 ppm. The nature of the natural solubility of chalcocite is not known.

A later experiment on the natural solubility of chalcocite was performed in a solution identical to those used in typical leach experiments except that nitrogen was used in place of oxygen. The analysis of the initial leach solution is given in Appendix A, Table X, Experiment Number 42. The concentration of copper dissolved was found to be

about 30 ppm after 30 minutes of leaching. A slight concentration increase (5 ppm) was observed during the next 540 minutes. Thus, all of the dissolution can be said to occur in the first 30 minutes.

Since the natural solubility is not related to the oxidation of the mineral and since the dissolution occurs in the first 30 minutes of reaction, no error will be introduced in the study of the oxidation reaction if the natural solubility is removed from the experimental data. This is equivalent to throwing out the first point and assuming the experiment started at 30 minutes elapsed time. Therefore, the natural solubility has been subtracted from the copper dissolution data in all calculations and graphical representations concerned with chalcocite oxidation.

Stoichiometry

The purpose of this series of experiments was to determine the coefficients of each reactant and product by finding the number of moles of reactant or product consumed or produced in a given period of time. The experimental procedure used was that described for reaction stoichiometry and rate of oxygen consumption.

Table VI is a tabulation of the stoichiometric data for seven experiments. The average mole ratios and their probable errors for H^{+}/Cu^{+2}, Cu^{+2}/O_2 and H^{+}/O_2 are respectively 2.047 ±0.025, 2.024 ±0.025 and 4.092 ±0.043.

Table VI

Stoichiometric Data for the Dissolution of Chalcocite in Oxygenated, Acid Solution

Expt. No.	H^+/Cu^{+2}	Cu^{+2}/O_2	H^+/O_2
4	1.931	2.058	3.942
5	2.026	2.016	4.092
7	2.020	2.131	4.310
10	1.992	2.085	4.150
12	2.236	2.095	4.302
13	2.022	1.926	3.900
14	2.105	1.854	3.951

Table VII

Tabulation of the Quantity of Sulfur Produced in Chalcocite Oxidation. All Sulfur is Reported as Sulfate.

Expt. No.	$(SO_4^{-2})_I$	$(SO_4^{-2})_F$	(SO_4^{-2})
2	.1263 M	.1269 M	.0006 M
37	.1509 M	.1525 M	.0006 M

These ratios can be rounded off respectively to 2, 2 and 4.

Determination of these ratios does not completely solve the reaction stoichiometry, because there are several reactions that chalcocite can undergo that produce the same ratios as those given above. The ratios do, however, rule out a number of reactions. Reactions (11), (12) and (16) are reactions that satisfy the mole ratios of 2, 2 and 4. It is possible to rule out reactions (12) and (16) on the

$$Cu_2S + \tfrac{1}{2}O_2 + 2H^+ = CuS + Cu^{+2} + H_2O \qquad (11)$$

$$Cu_2S + O_2 + 4H^+ = 2Cu^{+2} + S^o + 2H_2O \qquad (12)$$

$$CuS + \tfrac{1}{2}O_2 + 2H^+ = Cu^{+2} + S^o + H_2O \qquad (16)$$

basis of additional stoichiometric work.

During two other chalcocite oxidation experiments, the change in sulfur species in the leach solution was followed. The analytic procedure used was such that all sulfur species from S^{-2} to SO_4^{-2} would be included. In both cases, no significant change in soluble or free sulfur was detected. Table VII is a tabulation of this information. The subscripts I and F indicate respectively initial and final values. A carbon disulfide extraction of the leach residue (unreacted chalcocite) was performed to determine whether or not free sulfur was trapped in or on the surface of the leached chalcocite particles. Upon evaporation of the carbon disulfide, no free sulfur was visible. Free sulfur is apparently not formed during the dissolution reaction.

A final step in the stoichiometric work involved determing the identity of the reaction product. CuS was identified as a reaction product by the color of the leached surface and by x-ray diffraction identification. The details of this study are discussed in a section to follow.

Since neither free sulfur, nor any other sulfur species, can be found on the chalcocite surface or in the leach solution, reactions (12) and (16) can be ruled out as possible reaction paths. The identification of CuS as a reaction product, the absence of oxidized sulfur in the system and the mole ratios of 2, 2 and 4 for H^+/Cu^{+2}, Cu^{+2}/O_2 and H^+/O_2 respectively firmly support equation (11) as the only reaction occurring in the dissolution of chalcocite. Therefore, it is assumed that reaction (11) is the only reaction occurring in the dissolution process.

Rate of Oxygen Consumption

The purpose of this section of the study was to determine a general rate equation for the oxidation of chalcocite. The rate of reaction was followed by observing the consumption of oxygen in a closed system.

Figure 5 is a plot oxygen partial pressure vs. time for a typical oxygen consumption experiment. The initial leach solution contained 0.00104 M Cu^{+2} ion, 0.09967 M H^+ ion and 0.05088 M SO_4^{-2} ion. No other ionic species were present initially.

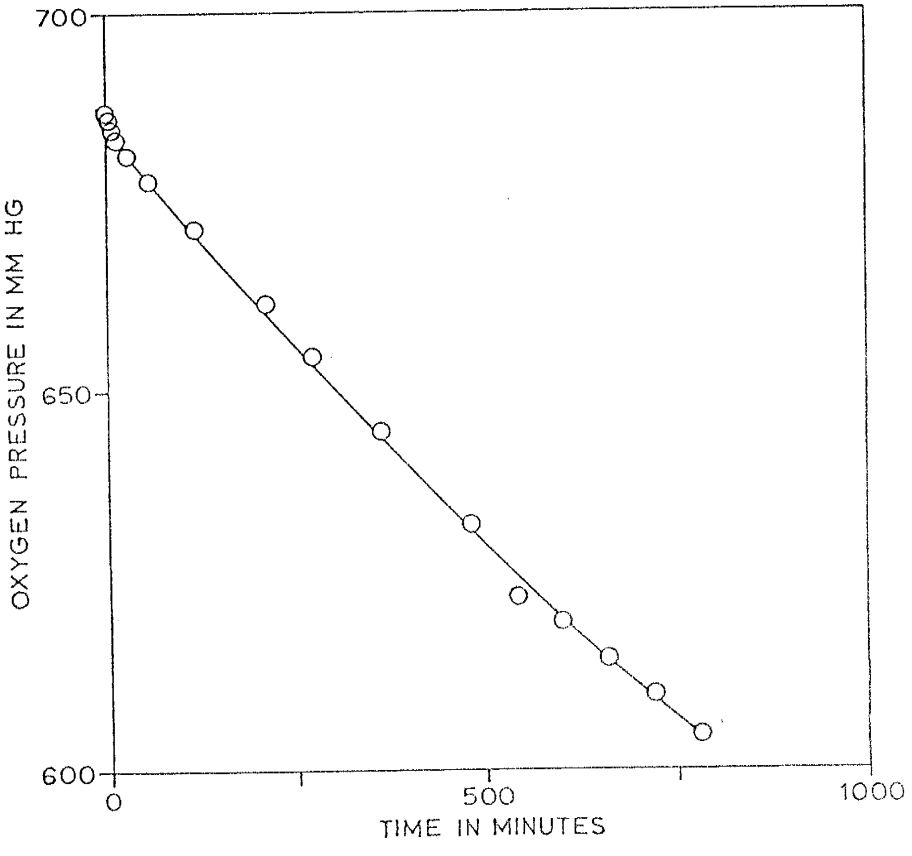

Figure 5. Oxygen Partial Pressure vs. Time for a Typical Oxygen Consumption Experiment.

Kinetic Analysis

One of the methods used to establish an experimental rate law involves postulation of a rate equation, manipulation of the equation to reduce it to one variable and time, integration of the equation and comparison of the experimental and predicted results.

Reaction (11) was assumed to be the one accompanying the oxidation of chalcocite. After considerable trial and error, the rate law given by equation (48) was assumed to

$$\frac{d(Cu^{+2})}{dt} = -\tfrac{1}{2}\frac{dP_{O_2}}{dt} = k(Cu^{+2})^0(H^+)^1(P_{O_2})^1 \qquad (48)$$

govern the reacting system. The development of this rate law is presented below.

The variable that was followed as a function of time was oxygen pressure. Therefore, the H^+ ion concentration must be expressed in terms of oxygen pressure. The H^+ ion concentration is related to the change in H^+ ion concentration by equation (49) where the subscript zero

$$(H^+) = (H^+)_o - \Delta(H^+) \qquad (49)$$

indicates an initial value. The concentration of dissolved O_2 is related to O_2 partial pressure by Henry's law which is represented by equation (50) where HK is Henry's constant.

$$(O_2) = 55.6\ P_{O_2}/HK \qquad (50)$$

The value of Henry's constant was found using equation (51)

$$HK = 1.973 \times 10^7 + 5.490 \times 10^5\ T \qquad (51)$$

where T is the absolute temperature. The change in H^+ ion concentration, $\Delta(H^+)$, is related through reaction stoichiometry to equation (52). Combination of equations (49), (50) and

$$(H^+) = 4\ \Delta(O_2) \tag{52}$$

(52) yield equation (53). Combination of equations (48)

$$(H^+) = (H^+)_o - (4)(55.6)(P_{O_2})_o/HK + (4)(55.6)(P_{O_2})/HK \tag{53}$$

and (53) yields equation (54) where $P_{O_2} = X$, $A = (H^+)_o$ -

$$\frac{dX}{dt} = -2k\ (A+BX)\ X \tag{54}$$

$222.4\ (P_{O_2})_o/HK$ and $B = 222.4/HK$. This equation can be integrated to yield equation (55) where C is the constant

$$\ln(A+BX) - \ln(X) = 2Akt + C \tag{55}$$

of integration.

A plot of $\ln(A+BX) - \ln X$ vs. time for the experimental data of Figure 5 should yield a straight line if the assumed rate equation is correct. Figure 6 is a plot of $\ln(A+BX) - \ln X$ vs. time. The curve produced is a straight line. Therefore, the oxidation of chalcocite in oxygenated, acid solution is first order with respect to both H^+ ion concentration and O_2 partial pressure and zero order with respect to Cu^{+2} ion concentration.

Summary

The data of the oxygen consumption experiments conform to the rate law given by equation (56). This result is

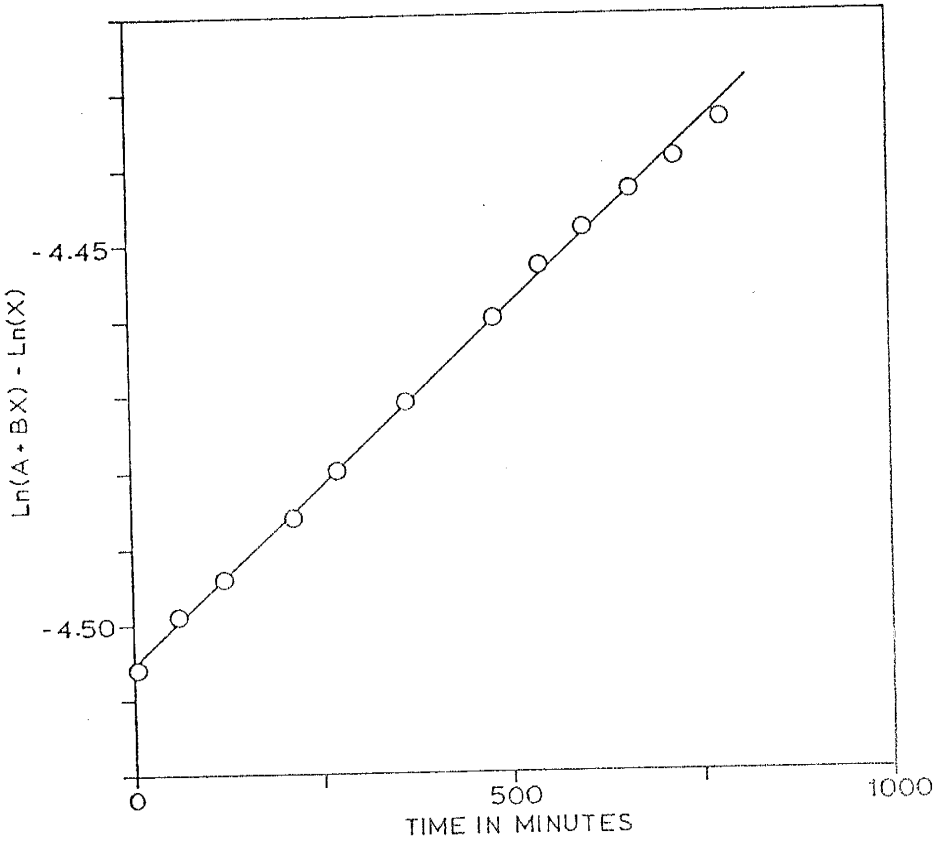

Figure 6. Ln(A+BX) - Ln(X) vs. Time for a Typical Oxygen Consumption Experiment.

$$\text{Rate} = k(P_{O_2})\ (H^+) \qquad (56)$$

substantiated by the work described in other sections.

Cupric Ion Concentration Change as a Measure of Rate

The overall purpose of this study was to determine the effect of different variables on the rate of chalcocite oxidation, to substantiate the general rate equation for the oxidation of chalcocite in oxygenated acid solution and to gain insight into a physico-chemical mechanism for the dissolution reaction. The experimental procedure was that described for cupric ion variation experiments. The experimental conditions and results for all of the experiments in this section are tabulated in Appendix A, Tables X and XI.

System Reproducibility

The purpose of this part of the study was to establish the accuracy with which an experiment could be reproduced. Three identical experiments were performed and compared to determine the extent of experimental error.

The stirring speed was 1150 RPM in each experiment. Figure 7 is a plot of cupric ion concentration vs. time for these three experiments. The average per cent standard deviation from the means was found to be ±4.22%.

The experimental conditions of this study were used as a basis for comparison in all other variable studies. The three experiments under discussion have been averaged at each experimental point to produce an average experiment which is used as a basis for comparison in all other studies.

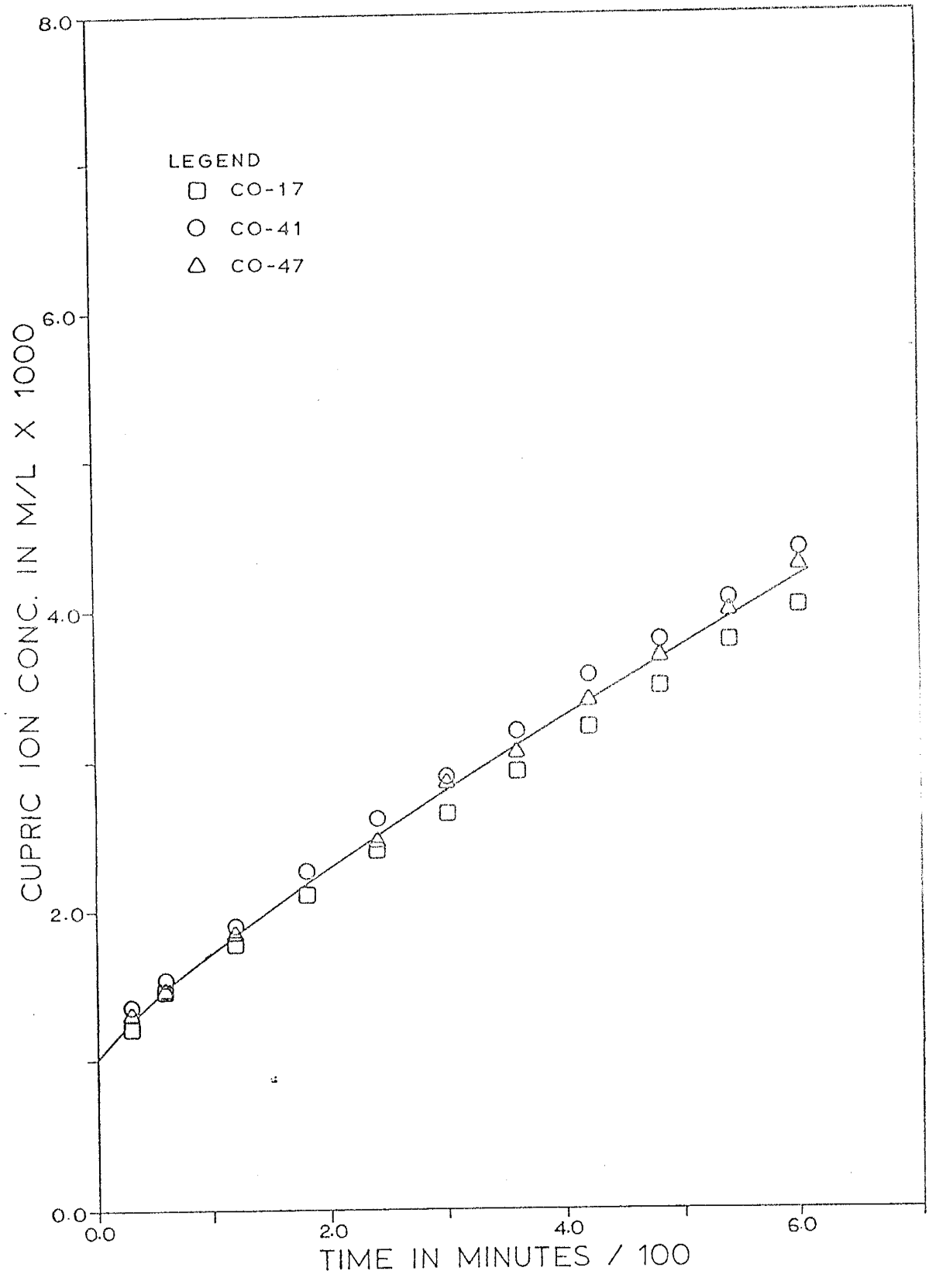

Figure 7. Cupric Ion Concentration vs. Time for Three Experiments Under the Same Experimental Conditions.

The Effect of Agitation

The purpose of this part of the study was to determine the role of agitation in the oxidation rate of chalcocite. Three experiments were performed with agitation as the only variable. Figure 8 is a plot of Cu^{+2} ion concentration vs. time for these experiments. There is no increase in reaction rate with increased stirring rate above 700 RPM The difference between the experiments at 1150 RPM and 700 RPM is within the expected experimental error. It has been assumed that diffusion occurs through a limiting boundary layer.

All other experiments were performed at the maximum stirring rate of 1150 RPM.

The Effect of Surface Area

The purpose of this work was to determine the effect of surface area on chalcocite dissolution. This was accomplished by performing three chemically identical experiments, but using three different weights of -48+65 mesh chalcocite. Experiments were carried out on 12.5, 25.0 and 50 grams of chalcocite which correspond respectively to 0.5, 1.0 and 2.0 per cent solids in the system.

The rate of a reaction is usually found to be first order with respect to surface area. The dissolution of chalcocite is no exception as shown by Figures 9 and 10. Figure 9 is a plot of cupric ion concentration vs. time for the three different weights of -48+65 mesh chalcocite. Figure 10 is a plot of log rate vs. log weight. The slope

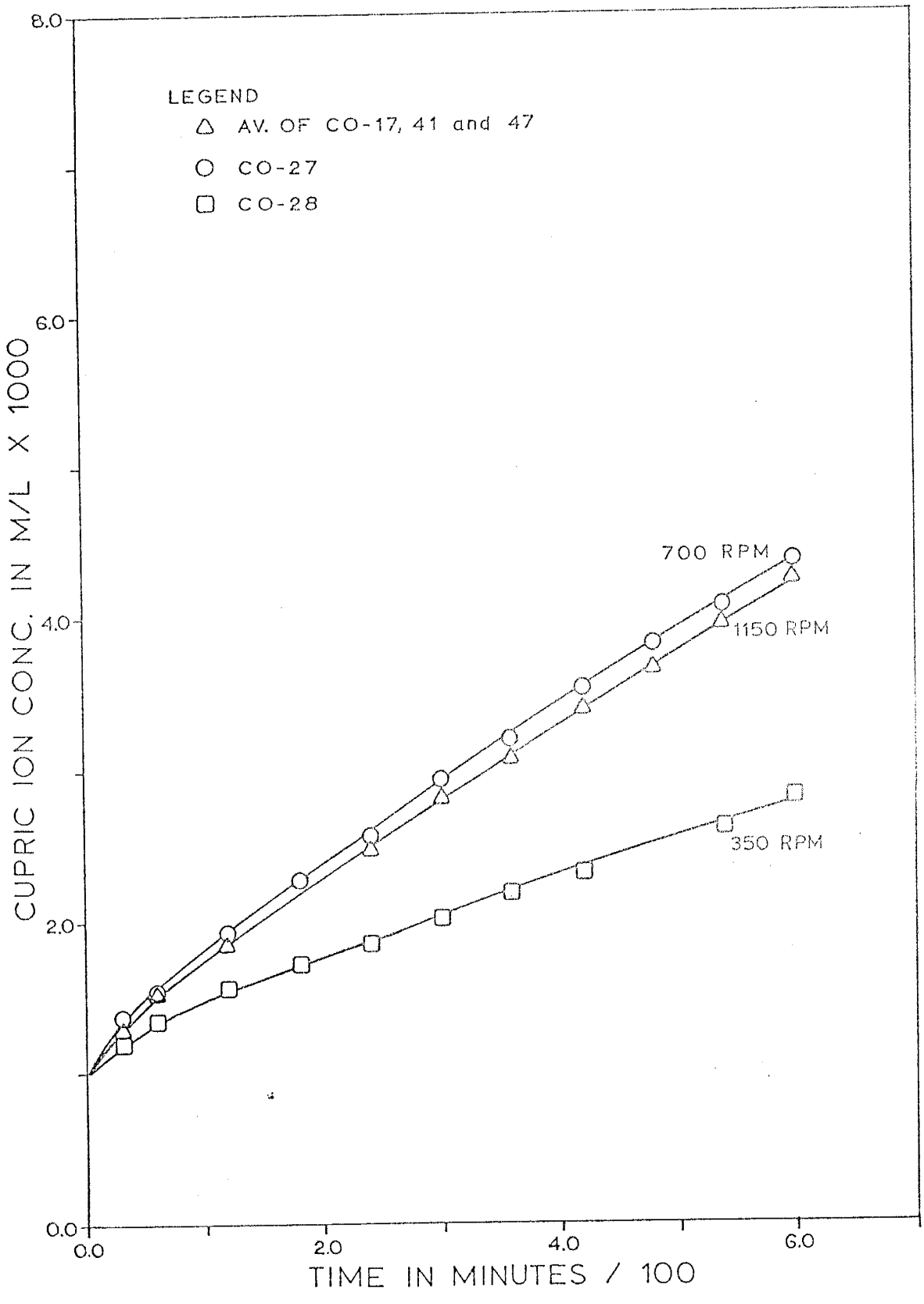

Figure 8. Cupric Ion Concentration vs. Time for Three Different Stirring Rates.

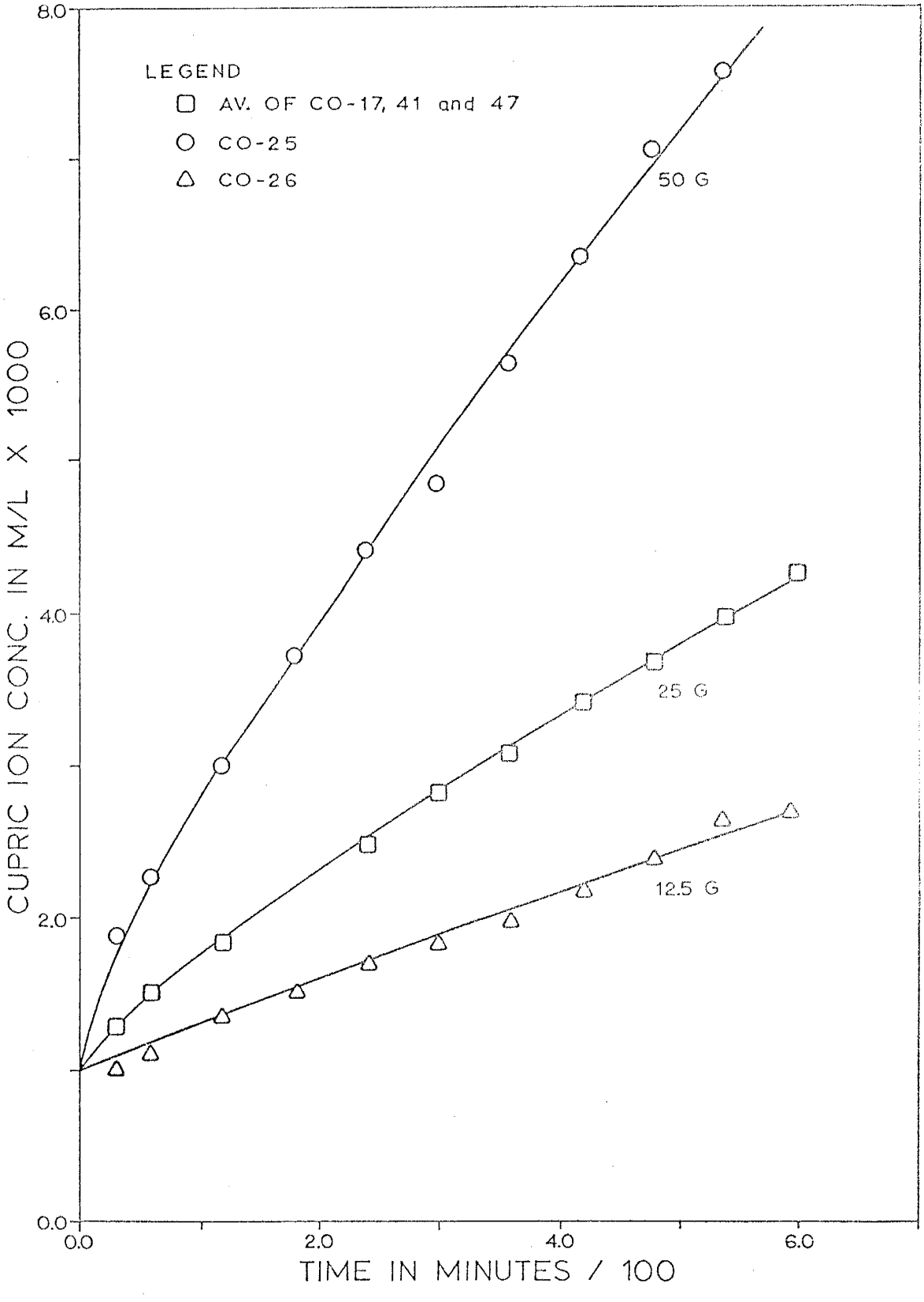

Figure 9. Cupric Ion Concentration vs. Time for Three Different Weights of -48+65 Mesh Chalcocite.

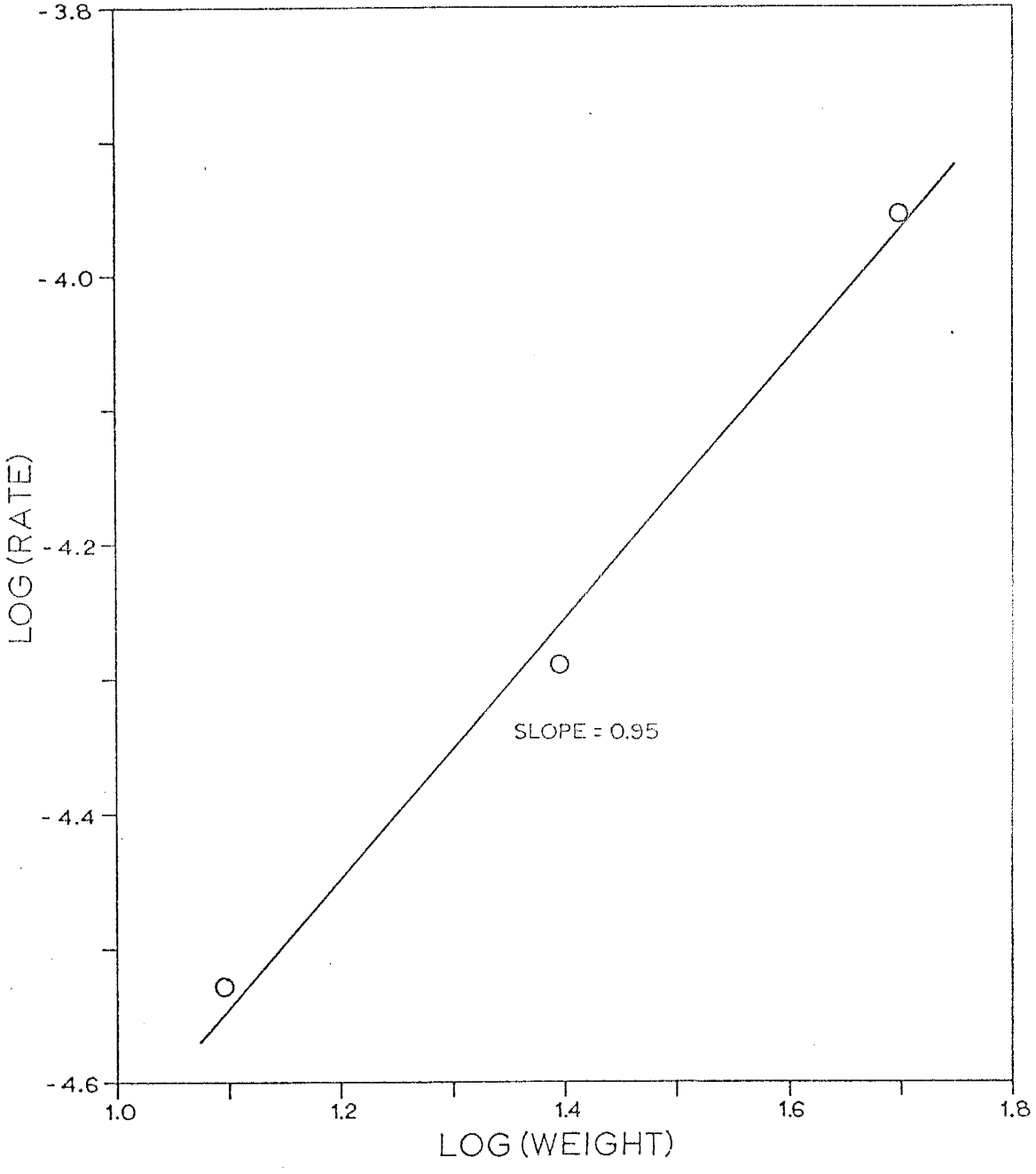

Figure 10. The Effect of Surface Area. Log(Rate) vs. Log(Weight).

of the line in Figure 10 was found to be 0.95 indicating that the rate of the reaction is first order with respect to the surface area of the chalcocite.

The Effect of O_2

The purpose of this section of the experimental work was to determine the order of the reaction with respect to oxygen partial pressure. This was accomplished by examining the effect of oxygen while all other variables were held constant.

Since all other variables were held at the same initial value, their constant effect can be included in a quasi-rate constant, k', and the rate equation for the system can be represented by equation (57). The exponent,

$$R = k'(P_{O_2})^a \qquad (57)$$

a, is the unknown reaction order for oxygen. The logarithmic form of this relation given by equation (58) is a

$$\log R = a \log P_{O_2} + \log k' \qquad (58)$$

line equation with a slope of a. Thus, a plot of log R vs. log P_{O_2} should yield a straight line of slope a.

The condition of the surface and the change in H^+ ion concentration during the reaction could effect this determination, so the rate selected from each experiment was at the same Cu^{+2} ion concentration (0.002250 M), not the same time. The rate of the reaction was determined from the

first derivative of a polynomial curve fitted through the experimental points of Figure 11. The details of the curve fitting procedure are given in Appendix B.

Figure 11 is a plot of Cu^{+2} ion concentration vs. time for four oxygen partial pressures. All other conditions were held constant. Figure 12 is a plot of log R vs. log P_{O_2} for which the slope is 0.96. Therefore, the reaction order with respect to oxygen partial pressure is 1. This is in agreement with the results of the oxygen consumption experiments.

Effect of Hydrogen Ion Concentration

The purpose of this portion of the work was to determine the order of the dissolution reaction with respect to H^+ ion over a wide concentration range. Three experiments were run with the initial concentration of H^+ and SO_4^{-2} ions as variables. Hydrogen ion is consumed in the reaction and its concentration changes with time during an experiment. However, it was shown in the stoichiometric study that the SO_4^{-2} ion concentration does not change during an experiment. Although the SO_4^{-2} ion concentration may influence the reaction rate, the effect is constant for a particular experiment and only the initial SO_4^{-2} ion concentration effects the rate of reaction.

Figure 13 is a plot of Cu^{+2} ion concentration vs. time for three different initial H^+ and SO_4^{-2} ion concentrations. Sulfate ion exerts an inverse effect on the rate of dissolution and neutralizes the effect of H^+ ion concentration.

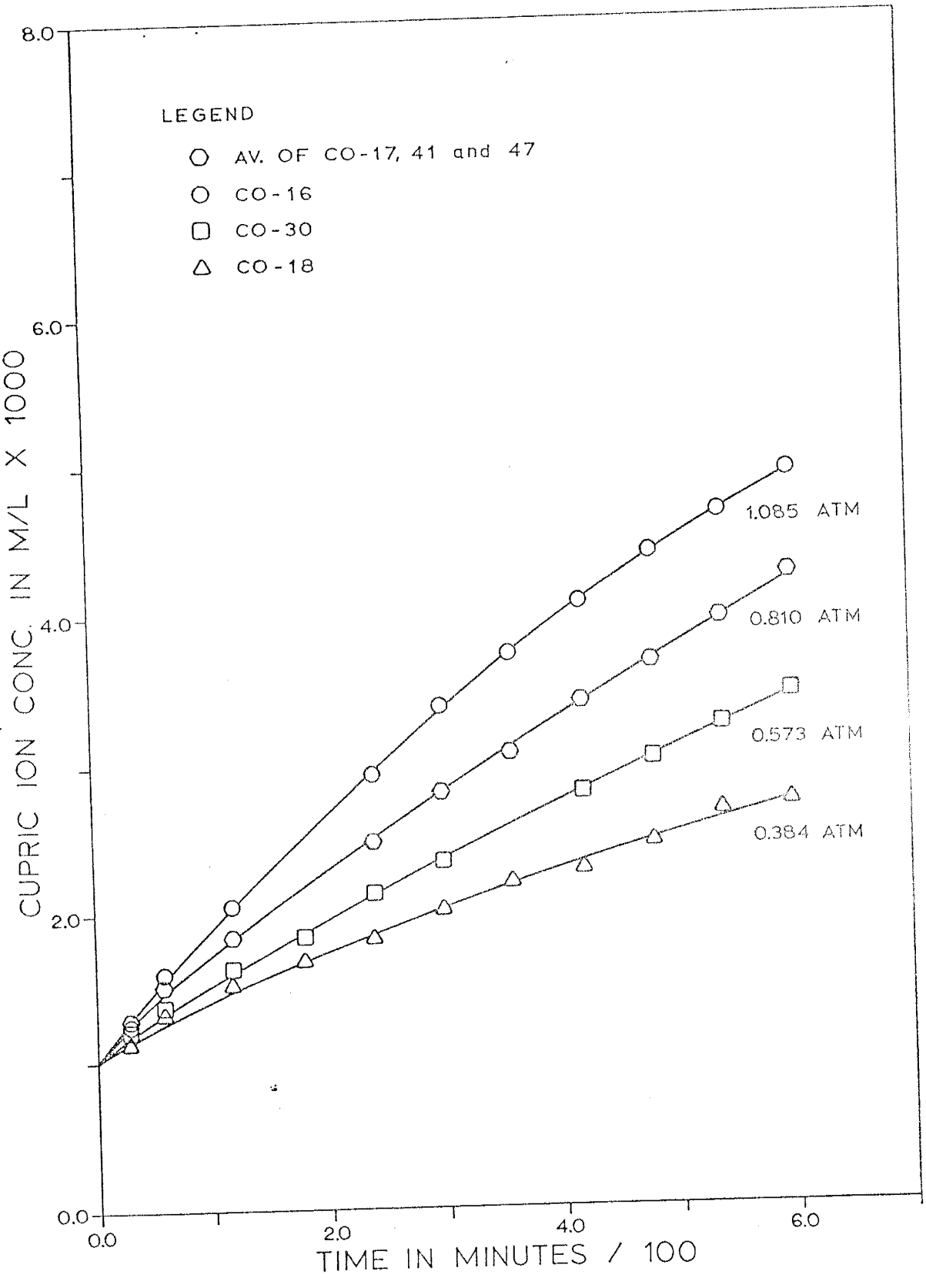

Figure 11. Cupric Ion Concentration vs. Time for Several Oxygen Partial Pressures.

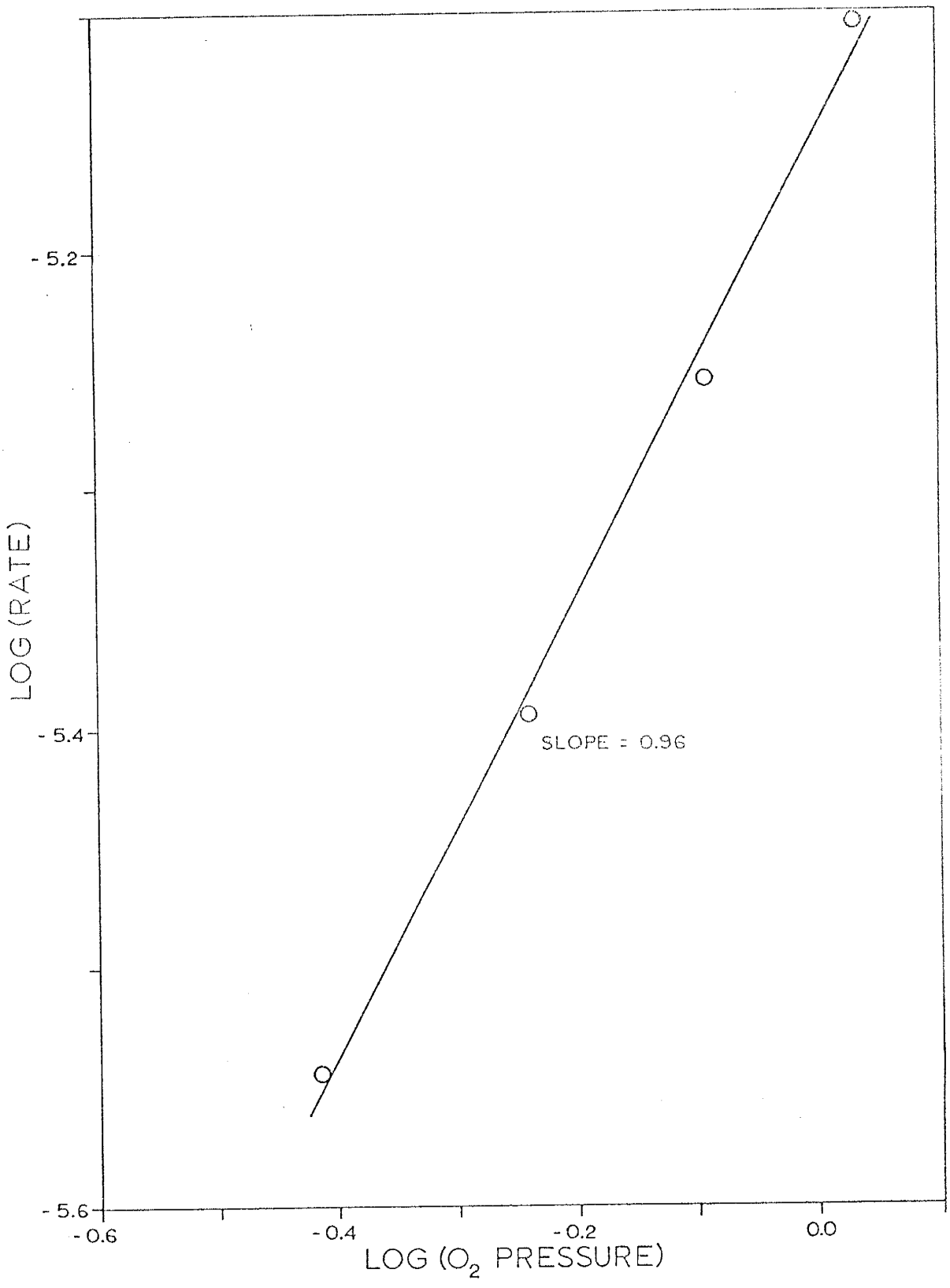

Figure 12. Log(Rate) vs. Log(P_{O_2}). Determination of Oxygen Reaction Order.

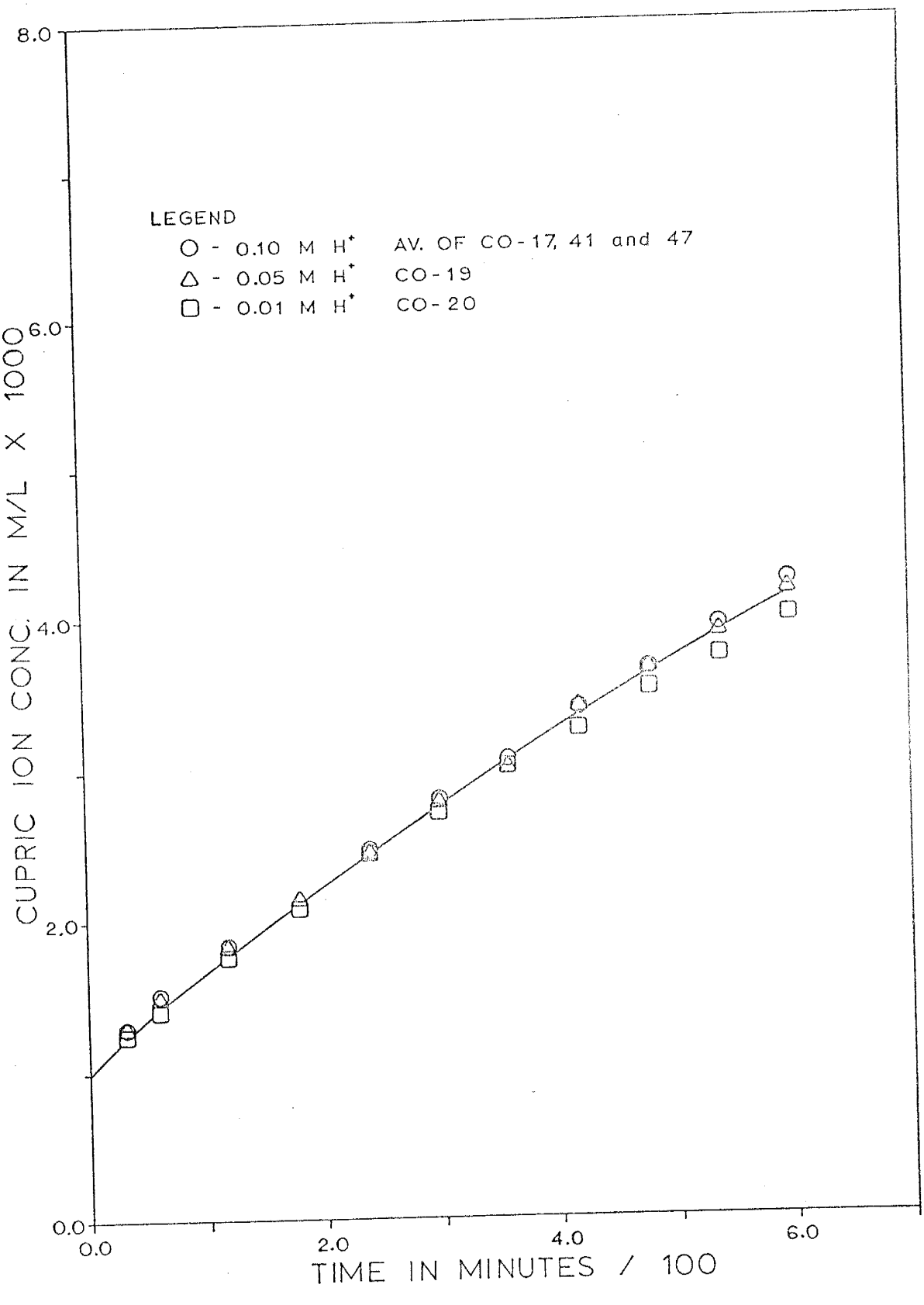

Figure 13. Cupric Ion Concentration vs. Time for Different Initial Hydrogen Ion Concentrations.

Since all variables except H^+ ion concentration were held constant during the course of each experiment, the rate equation for this part of the work can be expressed as equation (59) where k'' contains the constant effects

$$R = k'' (H^+) \tag{59}$$

of oxygen partial pressure and SO_4^{-2} ion concentration. The H^+ ion concentration is related to the Cu^{+2} ion concentration by equation (60). Combination of equations (59) and

$$(H^+) = (H^+)_o + 2(Cu^{+2})_o - 2(Cu^{+2}) \tag{60}$$

(60) yield equation (61) where $A = (H^+)_o + 2(Cu^{+2})_o$. Integration of this equation yields equation (62). A plot

$$\frac{d(Cu^{+2})}{dt} = k'' (A - 2(Cu^{+2})) \tag{61}$$

$$\ln (A - 2(Cu^{+2})) = -2k'' t + \ln C \tag{62}$$

of $\ln (A - 2(Cu^{+2}))$ vs. t will give a straight line if the assumed rate equation is correct. Figure 14 is a plot of these two variables for the experiment shown in Figure 13. The first order effect of H^+ ion concentration was found to hold over the H^+ ion concentration range 0.1 to 0.01 M.

The Effect of Sulfate

The purpose of this section of the study was to determine the order of the dissolution reaction with respect to sulfate ion concentration.

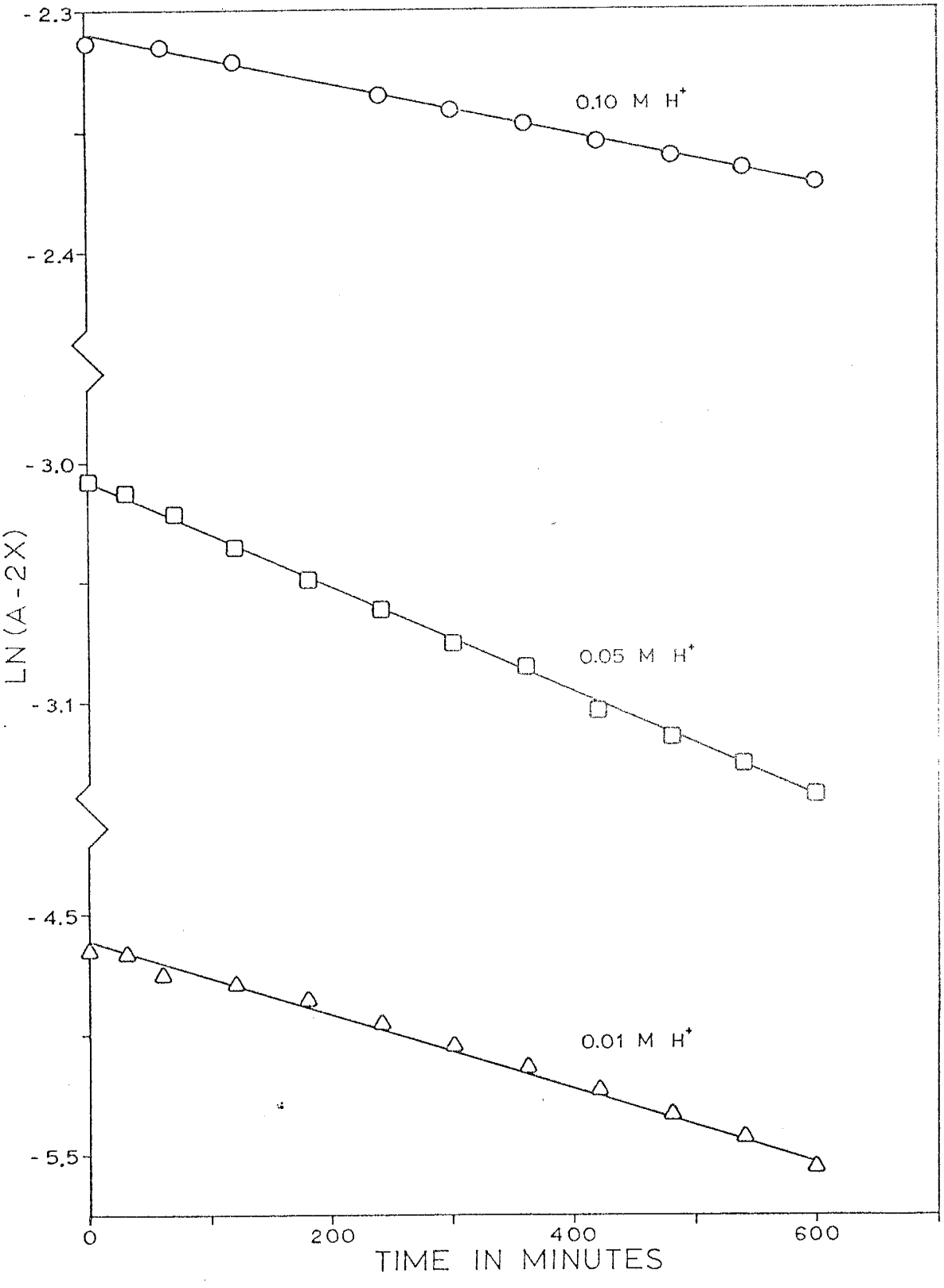

Figure 14. Ln(A-2X) vs. Time for Three Different H^+ Ion Concentrations. Hydrogen Ion Reaction Order.

In the last section the effect of sulfate was included in the quasi-rate constant since its effect is only a function of initial concentration. Equation (63) represents

$$k'' = k\,(SO_4^{-2})^b \qquad (63)$$

this situation where k'' is the quasi-rate constant of equation (62), k is a new rate constant containing the constant effect of oxygen and b is the unknown reaction order with respect to SO_4^{-2} ion concentration. The logarithmic form of this equation given by equation (64) is a line equation of slope b. A plot of log k'' vs. log

$$\log k'' = b \log (SO_4^{-2}) + \log k \qquad (64)$$

(SO_4^{-2}) should yield a straight line of slope b.

The slope of the lines in Figure 14 are equal to $-2k''$. Figure 15 was constructed using the k'' values determined from Figure 14. The slope of the line in Figure 15 was found to be -1.18. Therefore, reaction order with respect to sulfate is -1.18.

In other experiments sulfate ion was completely replaced by perchlorate and nitrate ions. Figure 16 is a plot of Cu^{+2} ion concentration vs. time showing the effects of SO_4^{-2}, ClO_4^- and NO_3^- ions. Sulfate ion depresses the reaction rate relative to the rate in ClO_4^- and NO_3^- solutions.

Summary of Kinetic Analysis

The analysis of the oxygen consumption experimental data indicated that the chalcocite oxidation reaction is

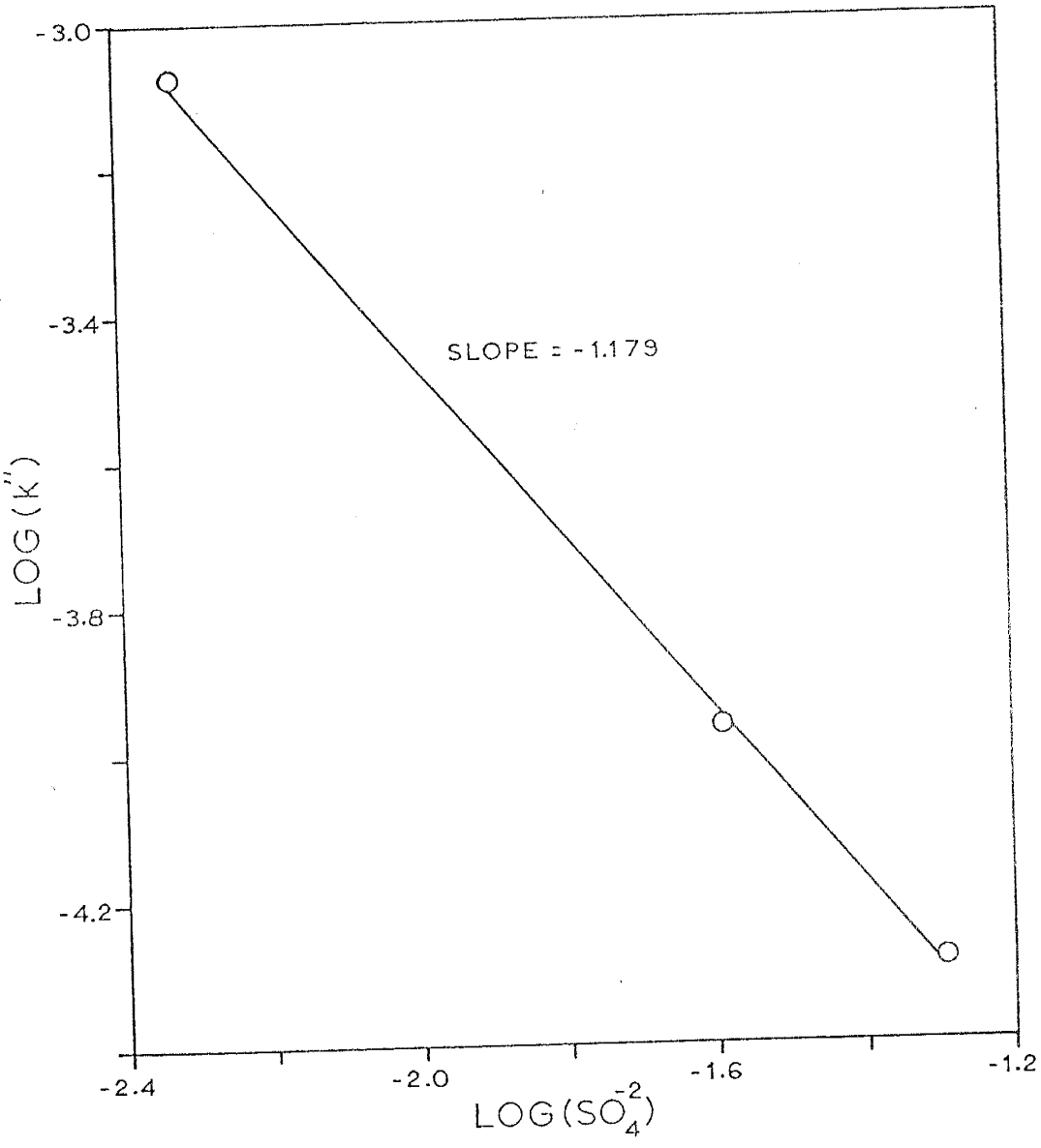

Figure 15. Sulfate Ion Reaction Order.

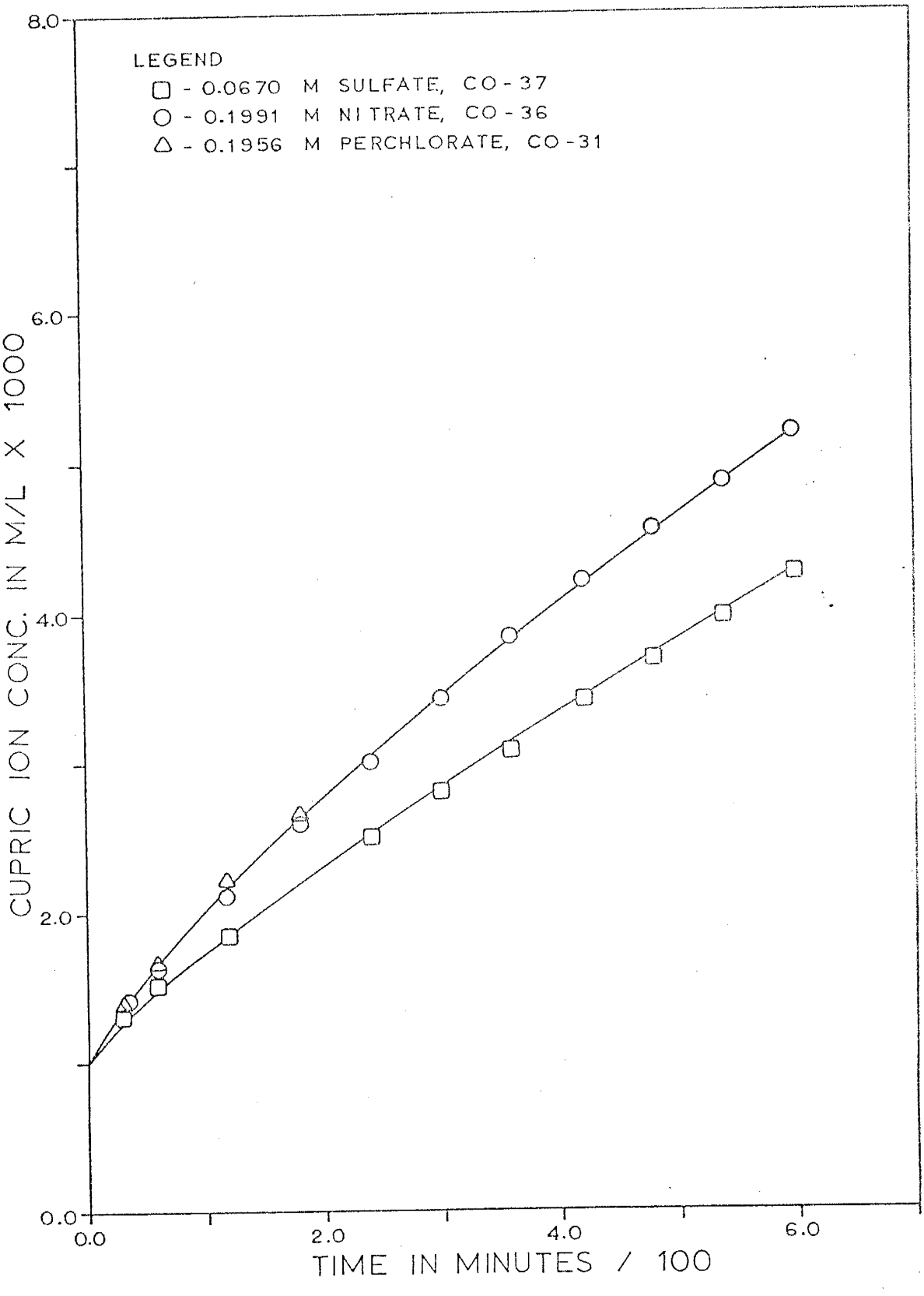

Figure 16. Cupric Ion Concentration vs. Time for Solutions Containing Sulfate, Nitrate and Perchlorate Ions.

first order with respect to H^+ ion concentration and oxygen partial pressure and zero order with respect to Cu^{+2} ion concentration.

Experiments at several constant oxygen partial pressures indicate that the oxidation reaction is first order with respect to oxygen pressure. Other experiments at various initial H^+ ion concentrations indicate that the reaction is first order with respect to H^+ ion concentration. The same H^+ ion experiments indicate that the reaction order with respect to sulfate ion is -1.18. These results support the rate law given by equation (65). This rate

$$R = k(P_{O_2})(H^+)(SO_4^{-2})^{-1.18} \qquad (65)$$

expression is valid over the H^+ ion concentration range 0.1 to 0.01 M, the SO_4^{-2} ion concentration range 0.005 to 0.05 M and the oxygen pressure range 1.085 to 0.384 atmospheres.

If the sulfate ion concentration does not vary from one experiment to another, then the rate law given by equation (56) is valid. The constant effect of SO_4^{-2} ion concentration is included in the rate constant.

The Effect of Temperature - Activation Energy

The purpose of this series of experiments was to determine the activation energy of the chalcocite dissolution reaction.

The rate constant for a reaction is related to temperature through the Arrhenius equation given as equation (66)

$$\frac{d \ln k}{dT} = \frac{E^*}{RT^2} \qquad (66)$$

where k is the rate constant, T is absolute temperature, R is the gas constant and E* is the activation energy of the reaction. The integrated form of this equation is given by equation (67). A plot of ln k vs. 1/T should

$$\ln k = \frac{-E^*}{RT} + \ln A \qquad (67)$$

give a straight line of slope -E*/R.

Values of k can be determined by solving equation (56) for k. The oxygen partial pressure is known and the H^+ ion concentration can be determined by using equation (60). Rate can be found as the derivative of the polynomial curve fitted through the experimental Cu^{+2} ion concentration vs. time data for each experiment. The rate selected from each experiment is taken at the same Cu^{+2} concentration (.004000 M), not the same time.

Figure 17 is a plot of cupric ion concentration vs. time for three different temperatures. Figure 18 is a plot of ln k vs. 1/T for these three experiments. The slope of the line gives an activation energy of 6.59 kcal/mole. Warren (1958) found an activation energy of 6.6 kcal/mole for the first stage of chalcocite dissolution at an oxygen pressure of 40 psi over the temperature range 100° to 200°C.

The significance of the activation energy is not clear. Burkin (1966) suggests that diffusion controlled reactions have activation energies of about 4 kcal/mole. A value of

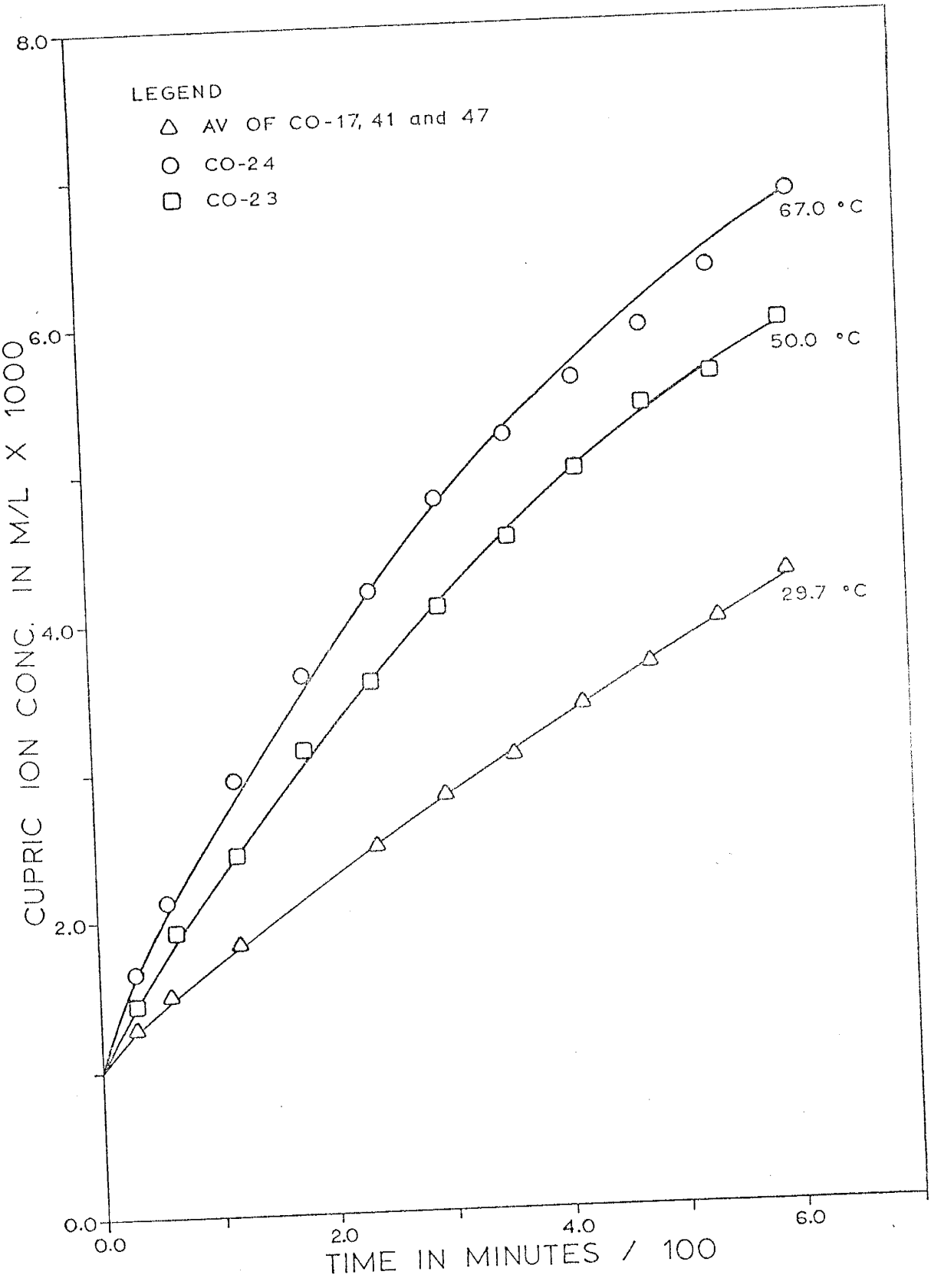

Figure 17. Cupric Ion Concentration vs. Time for Three Different Temperatures.

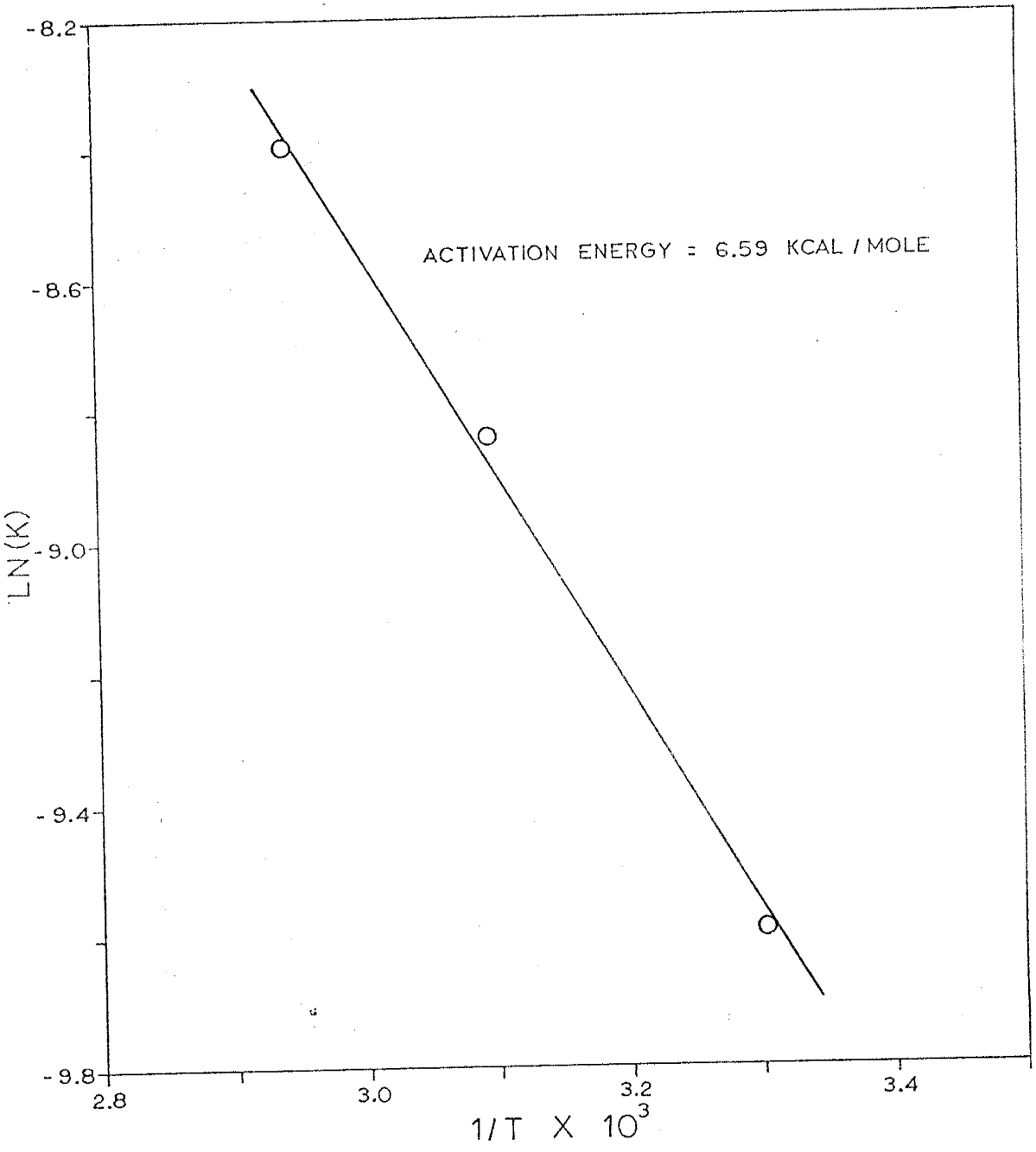

Figure 18. Determination of the Activation Energy for the Dissolution of Chalcocite.

6.6 kcal/mole could indicate either diffusion or chemical rate control.

The Effect of Chloride and Bromide Ions

The purpose of this portion of the study was to determine the effect of chloride and bromide ions on the dissolution of chalcocite.

The reaction mechanism involves the existence of Cu^{+1} ion as an intermediate. The cuprous ion normally undergoes spontaneous disproportionation to form Cu^{+2} and metallic copper, and therefore, the Cu^{+1} ion equilibrium concentration in solution is very small. The halide ions all have the ability to selectively complex Cu^{+1} ion in preference to Cu^{+2} ion. The stability constants for $CuCl_2^-$, $CuCl^+$, $CuBr_2^-$ and $CuBr^+$ given by Yatsimirskii and Vasil'ev (1960) are respectively 2.00×10^5, 1.30, 7.69×10^5 and 2.0. The larger the value of the stability constant, the greater the stability of the complex. Thus, Cu^{+1} complexes are clearly more stable than Cu^{+2} complexes. The presence of Cl^- or Br^- ions should stabilize Cu^{+1} ion and increase its equilibrium concentration in solution.

Equation (30) of the reaction mechanism proposes the existence of a Cu^{+1} ion at the surface of the mineral. If the equilibrium concentration of this species can be increased, then the reaction rate should increase if equation (30) is the rate controlling reaction.

Figure 19 is a plot of Cu^{+2} ion concentration vs. time for three experiments showing the effect of chloride and

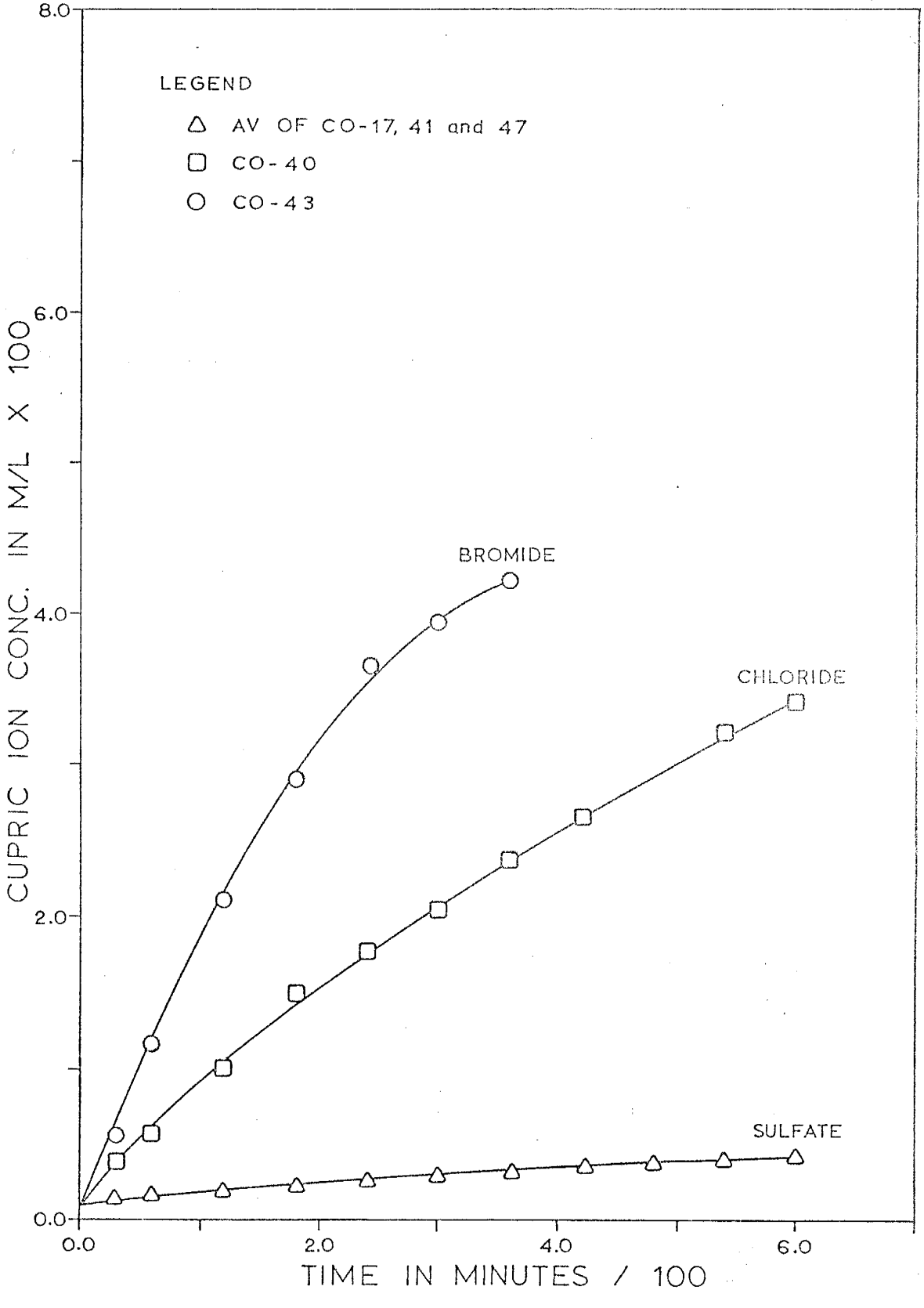

Figure 19. Cupric Ion Concentration vs. Time for Several Different Anions.

bromide ions. The presence of halide ions increases the reaction rate by a factor of about 100.

The Identification of CuS

The leached chalcocite recovered from the chloride and bromide dissolution experiments no longer appeared to be chalcocite. The mineral grains were a definite deep blue in color and could easily be mistaken for covellite. Sato (1960a), Kuxmann and Biallab (1969), Stanczyk and Rampacek (1966) and Gerlach and Pawleck (1968) have postulated CuS as a reaction intermediate during chalcocite dissolution. However, none of these investigators isolated and identified the intermediate. Since the color of the leached chalcocite was definite, it was clear that it was more than a superficial coating. Therefore, it was decided that the product might be identified using x-ray powder diffraction.

A sample of -200 mesh chalcocite was leached for 530 minutes in a solution containing .001 M Cu^{+2}, .1000 M H^{+}, .0970 M Na^{+} and .1980 M Br^{-}. The solids that remained were recovered, washed thoroughly and air dried. A sample of unleached -200 mesh chalcocite and a sample of the leached -270 mesh chalcocite were subjected to x-ray diffraction analysis. The conditions of the analysis for each sample were identical. The results of the x-ray analyses are given in Appendix A, Tables XII and XIII and are shown graphically in Figure 20. Figure 20 is a photographically reduced tracing of the two x-ray diffraction spectra.

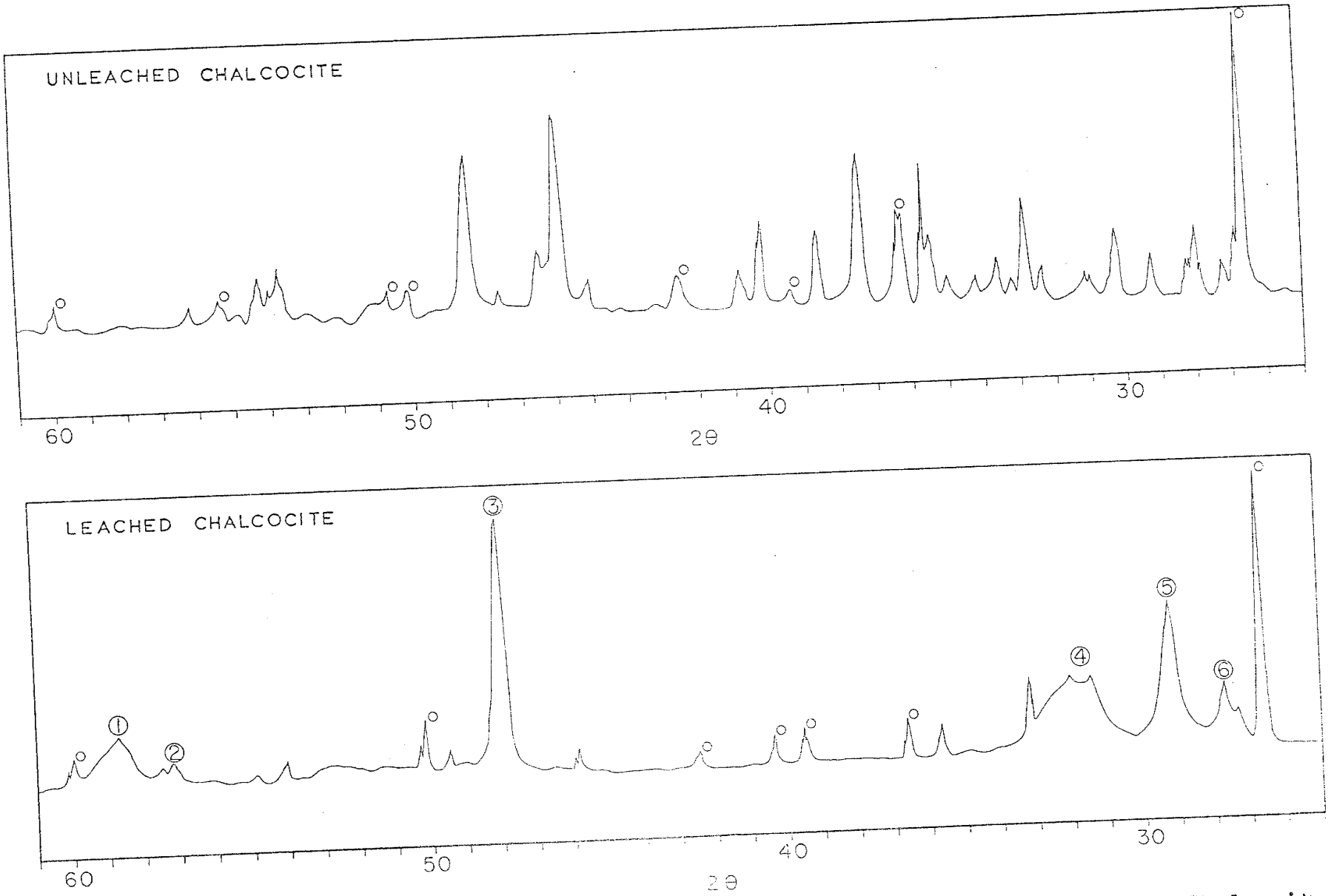

Figure 20. Comparison of the X-Ray Diffraction Spectra for Unleached and Leached Chalcocite.

The peaks in Figure 20 are identified as follows. All unmarked peaks belong to chalcocite, those marked with a circle are quartz and those indicated with a number are CuS.

Figure 20 exhibits several interesting features. The chalcocite spectra in the leached material is very weak compared to the spectra of unleached chalcocite. The quartz lines are essentially the same in both cases. Peaks 1 and 2 of the leached material can be clearly identified with covellite. Peak 3 can be identified with either Cu_2S or CuS. However, the peak does not exist in the unleached chalcocite spectra and there is no reason to believe that leaching would enhance this one peak while in general destroying all others. Peak 3 most probably belongs to CuS. Peak 4 corresponds to two very intense CuS peaks although no definite peak exists at position 4. Peak 5 could belong to either Cu_2S or CuS, but since Cu_2S seems to be depressed in other areas, this peak is attributed to CuS. Peak 6 is a CuS diffraction peak.

These results clearly indicate that covellite is a reaction product of chalcocite dissolution.

Summary

The purpose of this section of the study was to determine the rate of chalcocite dissolution as a function of agitation, surface area, oxygen partial pressure, H^+ ion concentration, SO_4^{-2} ion concentration and halide ion concentration, substantiate the general rate equation and find support for a physico-chemical reaction mechanism.

The system reproducibility was found to be 4.22%. Increased agitation produced higher reaction rates up to 700 RPM. All experiments were performed at 1150 RPM so that agitation was not a variable. Reaction rate was found to be first order with respect to surface area at constant particle size. The dissolution reaction was found to be first order with respect to oxygen partial pressure and H^+ ion concentration. The reaction order with respect to SO_4^{-2} ion was found to be -1.18. The reaction rate was found to be controlled by an activation energy of 6.6 kcal/mole. Both Cl^- and Br^- ions caused increases in reaction rate. The product of the dissolution reaction was identified as CuS by x-ray diffraction.

A Physico-Chemical Reaction Mechanism

The only reaction that is occurring in the dissolution of chalcocite is reaction (11). The dissolution is

$$Cu_2S + \tfrac{1}{2}O_2 + 2H^+ = CuS + Cu^{+2} + H_2O \qquad (11)$$

governed by the experimental rate law represented by equation (56). Any mechanism proposed for chalcocite

$$R = k\,(P_{O_2})\,(H^+) \qquad (56)$$

dissolution must be consistent with equations (11) and (56).

When the rate controlling reaction is assumed to be dissolution of O_2 in the solution, the rate law is given by

equation (41). This rate law is not in agreement with

$$R = k_{40}(O_2) \tag{41}$$

equation (56), and therefore, the rate is not controlled by O_2 transport into the solution.

Reaction rate control by sorption of O_2 on the mineral surface leads to the rate law given by equation (44).

$$R = \frac{k_{28}\, k_{29}}{k_{-28}} (O_2) \tag{44}$$

Again, this rate law is not consistent with equation (56). Thus, rate control is apparently not due to O_2 sorption.

If the rate controlling reaction is the first reduction step for O_2, the rate law is given by equation (47). This

$$R = \frac{k_{28}\, k_{29}\, k_{30}}{k_{-28}\, k_{29}} (O_2)\, (H^+) \tag{47}$$

rate law is the same as equation (56) with $k = \frac{k_{28}\, k_{29}\, k_{30}}{k_{-28}\, k_{29}}$.

Therefore, the rate of the reaction is apparently governed by reaction (30) of the reaction sequence.

The reaction mechanism given by equations (28) through (39) is postulated as a physico-chemical mechanism of chalcocite dissolution.

$$Cu_2S\} \overset{\text{fast}}{\rightleftharpoons} Cu_{2-x}S\}Cu^{+1} \tag{28}$$

$$Cu_{2-x}S\}Cu^{+1} + O_2\ (aq) \overset{\text{fast}}{\rightleftharpoons} Cu_{2-x}S\}Cu^{+1}\text{--}O_2 \tag{29}$$

$$Cu_{2-x}S\}Cu^{+1}\text{--}O_2 + H^+ \overset{\text{slow}}{\longrightarrow} Cu_{2-x}S\}Cu^{+2}\text{--}HO_2 \tag{30}$$

$$Cu_2S\ \ Cu_{2-x}S\}Cu^{+2}\text{--}HO_2 \overset{\text{fast}}{\rightleftharpoons} Cu_2S\ \ CuS\}Cu^{+1}\text{--}HO_2 + Cu^{+2} \tag{31}$$

$$Cu_2S\ \ CuS\}Cu^{+1}\text{--}HO_2 + H^+ \overset{\text{fast}}{\longrightarrow} Cu_2S\ \ CuS\}Cu^{+2}\text{--}H_2O_2 \tag{32}$$

$$Cu_2S\ \ CuS\}Cu^{+2}\text{--}H_2O_2 \overset{\text{fast}}{\rightleftharpoons} Cu_{2-x}S\ \ CuS\}Cu^{+1}\text{--}H_2O_2 + Cu^{+2} \tag{33}$$

$$Cu_{2-x}S\ \ CuS\}Cu^{+1}\text{--}H_2O_2 + H^+ \overset{\text{fast}}{\longrightarrow} Cu_{2-x}S\ \ CuS\}Cu^{+2}\text{--}OH + H_2O \tag{34}$$

$$Cu_2S\ \ Cu_{2-x}S\ \ CuS\}Cu^{+2}\text{--}OH \overset{\text{fast}}{\rightleftharpoons} Cu_2S\ \ CuS\ \ CuS\}Cu^{+1}\text{--}OH + Cu^{+2} \tag{35}$$

$$Cu_2S\ \ CuS\ \ CuS\}Cu^{+1}\text{--}OH + H^+ \overset{\text{fast}}{\longrightarrow} Cu_2S\ \ CuS\ \ CuS\}Cu^{+2} + H_2O \tag{36}$$

$$Cu_2S\ \ CuS\ \ CuS\}Cu^{+2} \overset{\text{fast}}{\rightleftharpoons} Cu_{2-x}S\ \ CuS\ \ CuS\}Cu^{+1} + Cu^{+2} \tag{37}$$

$$Cu_{2-x}S\ \ CuS\ \ CuS\}Cu^{+1} + O_2\ (aq) \overset{\text{fast}}{\rightleftharpoons} Cu_{2-x}S\ \ CuS\ \ CuS\}Cu^{+1}\text{--}O_2 \tag{38}$$

$$\vdots$$

$$CuS\ \ CuS\ \ CuS\ \ CuS\}Cu^{+2} \overset{\text{fast}}{\rightleftharpoons} CuS\ \ CuS\ \ CuS\ \ CuS\} + Cu^{+2} \tag{39}$$

SUMMARY AND CONCLUSIONS

Electrode Potential of Chalcocite

The electrode potential of chalcocite was found to be 0.462 V. This potential corresponds to reaction (9)

$$Cu_2S = CuS + Cu^{+2} + 2e \qquad (9)$$

which has a theoretical electrode potential of 0.530 V.

Natural Chalcocite Solubility

Chalcocite was found to have a limited, finite solubility in a non-oxidizing solution. The experimental solubility was not in agreement with the solubility product of chalcocite. The copper that was dissolved was apparently not due to oxidation in solution and was not the result of surface oxidation during grinding. The solubility amounts to 3.1×10^{-5} moles per gram of -48+65 mesh chalcocite. The nature of the solubility phenomenon is not known.

Stoichiometry

The average mole ratios of H^+/Cu^{+2}, Cu^{+2}/O_2 and H^+/O_2 were found to be respectively 2, 2 and 4. No sulfur species was produced during the dissolution of chalcocite. CuS was found to be a reaction product. All of these findings support reaction (11) as the only dissolution

$$Cu_2S + \tfrac{1}{2}O_2 + 2H^+ = CuS + Cu^{+2} + H_2O \qquad (11)$$

reaction occurring in an oxygenated sulfuric acid solution.

Rate of Oxygen Consumption

The dissolution process in oxygenated acid solution was found to follow the rate law given by equation (56)

$$R = k\,(P_{O_2})\,(H^+) \qquad (56)$$

Cupric Ion Concentration Change as a Measure of Rate

The system reproducibility was found to be 4.22%. The effect of surface area at constant particle size was found to be first order. Increased agitation was found to increase the reaction rate up to a stirring speed of 700 RPM. There was no further increase in reaction rate above 700 RPM.

The reaction was found to be first order with respect to both oxygen partial pressure and H^+ ion concentration. This is in agreement with the results found in the oxygen consumption experiments. These results substantiate equation (56) as the rate law for the dissolution of chalcocite. In addition the initial SO_4^{-2} ion concentration was found to have a reaction order of -1.18. The activation energy for the dissolution of chalcocite was found to be 6.6 kcal/mole. The activation energy is attributed to a chemically controlled process.

When sulfate was replaced by either perchlorate or nitrate, the reaction rate increased. Chloride and bromide ions were found to increase the reaction rate by a factor of about 100 with respect to the rate in sulfate, perchlorate or nitrate solutions. The increase in reaction rate is attributed to complexing of the Cu^{+1} ion by Cl^- or Br^- ion.

The reaction product formed during dissolution of chalcocite was found to be CuS.

A Physico-Chemical Reaction Mechanism

The reaction sequence given by equations (28) through (39) is proposed as a mechanism for chalcocite dissolution in oxygenated, acid solution. Reactions (28) and (29) are considered to establish rapid equilibria and reaction (30) is considered to be the rate controlling reaction. The first three reactions in the sequence lead to a rate equation of the same form as equation (56).

Conclusions

The only reaction accompanying the dissolution of chalcocite in oxygenated sulfuric acid solution is given by equation (11). The dissolution process is governed

$$Cu_2S + \tfrac{1}{2}O_2 + 2H^+ = CuS + Cu^{+2} + H_2O \qquad (11)$$

by the rate law represented by equation (56). This rate law is valid over the H^+ ion concentration range 0.01 to

0.1 M and the oxygen pressure range of 1.085 to 0.384 atmospheres. The activation energy for the dissolution

$$R = k(P_{O_2})\ (H^+) \qquad (56)$$

reaction is 6.6 kcal/mole. The rate controlling step is considered to be chemical in nature.

The reaction rate is first order with respect to surface area. Sulfate ion has a -1.18 order effect on the reaction rate and depresses the reaction rate relative to the rate in perchlorate or nitrate solutions. The presence of chloride or bromide ion in the solution causes a 100 fold increase in reaction rate.

The reaction mechanism consistent with all of the experimental findings is given by equations (28) through (39).

RECOMMENDATIONS

The Effect of Sulfate

The exact effect that SO_4^{-2} ion has on the chalcocite dissolution reaction was not determined. The general effect of SO_4^{-2} ion was to depress the reaction rate. It is the opinion of this investigator that the non-oxidative solubility of chalcocite, the effect of sulfate and the equilibrium between S^{-2} in the mineral surface and oxy-sulfur species in the solution are directly related. A study of these phenomena could yield useful information on the surface chemistry of sulfide minerals.

The Physical Aspects of the Reaction Mechanism

The proposed reaction mechanism includes both physical and chemical phenomena. The solid state reactions of this mechanism were not substaniated by experimental results, but were instead compared to the results of another leaching study (Dutrizac et al., 1970).

A study of the stoichiometry and the crystal structure of Cu_2S as it is leached could produce information leading to a theory on the solid state transformations occurring during aqueous, oxidative dissolution of sulfide minerals. The stoichiometry can be determined using conventional chemical analysis and electron microprobe analysis.

Structure studies can be carried out using x-ray diffraction techniques.

The Chemical Aspects of the Reaction Mechanism

The chemical steps in the reaction mechanism are concerned primarily with the reduction of oxygen. The first step in this reduction has been considered as rate controlling. A detailed kinetic study of the reduction of oxygen in various aqueous environments with the concentration of cupric, sulfate, perchlorate, nitrate, chloride and bromide ions as variables could indicate whether or not the rate controlling steps in oxygen reduction and chalcocite oxidation are the same.

REFERENCES

Burkin, A.R. (1966) The Chemistry of Hydrometallurgical Processes, D. Van Nostrand Inc., Princeton, New Jersey.

Dutrizac, J.E., Mac Donald, R.J.C. and Ingraham, T.R. (1970) The Kinetics of Dissolution of Bornite in Acidified Ferric Sulfate Solutions, Metallurgical Trans., v. 1, pp. 125-31.

Gerlack, J. and Pawlek, F. (1968) On the Kinetics of Pressure Leaching of Metal Sulfides and Ores, Paper presented at the Annual Meeting of the AIME, New York, N.Y., Feb. 25-29, 1968.

Hodgman, C.D., Weast, R.C. and Selby, S.M. (1960) Handbook of Physics and Chemistry, The Chemical Rubber Publishing Co., Cleveland, Ohio.

Huffman, R.E. and Davidson, N. (1956) Kinetics of the Ferrous Iron-Oxygen Reaction in Sulfuric Acid Solution, J. Am. Chem. Soc., v. 78, pp. 4836-42.

Kuxmann, V.U. and Biallab, H. (1969) Studies on Copper Matte Electrolysis, Erzmetall, v. 22, #2, pp. 53-64. (German)

Latimer, W.M. (1952) Oxidation Potentials, Prentice-Hall Inc., Englewood Cliffs, N.J.

Olson, A.R., Koch, C.H. and Pimentel, G.C. (1956) Introductory Quantitative Chemistry, W.H. Freeman and Company, San Francisco.

Sato, M. (1960) Oxidation of Sulfide Ore Bodies, I. Geochemical Environments in Terms of Eh and pH, Econ. Geol. v. 55, pp. 938-61.

Sato, M. (1960a) Oxidation of Sulfide Ore Bodies, II. Oxidation Mechanisms of Sulfide Minerals at 25°C, Econ. Geol., V. 55, pp. 1202-31.

Stanczyk, M.H. and Rampacek, C. (1966) Oxidation Leaching of Copper Sulfides in Acidic Pulps at Elevated Temperatures and Pressures, USBM Report of Investigations 6193.

Sullivan, J.D. (1930) Chemistry of Leaching Chalcocite, USBM Technical Paper 473.

Warren, I.H. (1958) Acid Pressure Leaching of Chalcopyrite, Chalcocite and Covellite, Australian J. Appl. Sci., v. 9, pp. 36-51.

Worthing, A.G. and Geffner, J. (1943) Treatment of Experimental Data, John Wiley and Sons, Inc., New York.

Yatsimirskii, K.B. and Vasil'ev, V.P. (1960) Instability Constants of Complex Compounds, Consultants Bureau, New York.

Appendix A. Tables of Chalcocite Dissolution Data

Table VIII

Tabulation of Chalcocite Electrode Potential Data.

Elapsed Time (Min)	Cell Potential (V)	Oxygen Pressure (atm)
0		0.812
15	0.13188	0.812
30	0.13162	0.812
45	0.13170	0.812
60	0.13150	0.812
145	0.13434	0.814
900	0.13365	0.815
1180	0.14017	0.811
1470	0.13950	0.812
2302	0.13215	0.814
2560	0.13369	0.812
2585	0.13734	0.812
2725	0.13412	0.812
3000	0.12988	0.813
3740	0.12988	0.815
4050	0.13207	0.811
4430	0.13168	0.811
5300	0.13177	0.810
6700	"	0.812
8075	"	0.806
8505	"	0.803
9495	"	0.809
9755	"	0.805
17070	"	0.803
18145	"	0.809
18265	"	0.809

Table IX

Oxygen Partial Pressure as a Function of Time During Chalcocite Oxidation

Elapsed Time (Min)	O_2 Pressure (mm Hg)
2.5	686.9
5.0	686.1
10.0	684.6
16.0	683.3
30.0	681.1
60.0	677.7
120.0	671.3
210.0	661.5
270.0	654.7
360.0	644.6
480.0	632.5
540.0	624.6
600.0	619.6
660.0	614.5
720.0	609.8
780.0	604.5

Table X

Initial Conditions for the Rate of Chalcocite Dissolution.

Expt. No.	Fig. No.	Temp. (°C)	O_2 pp (atm)	(H^+) (M)	(Cu^{+2}) (M)	(Na^+) (M)	(SO_4^{-2}) (M)	(ClO_4^-) (M)	Other (M)	I (M)
CO-16	11	30.0	1.085	0.10000	0.00103	0.04600	0.05103	0.04600		0.2001
CO-17	7	28.5	0.812	0.10000	0.00103	0.04600	0.05103	0.04600		0.2001
CO-18	11	30.0	0.384	0.10000	0.00103	0.04600	0.05103	0.04600		0.2001
CO-19	13	30.0	0.806	0.04940	0.00102	0.12100	0.02572	0.12100		0.1992
CO-20	13	30.0	0.810	0.00963	0.00104	0.18100	0.00586	0.18100		0.1999
CO-23	17	50.0	0.724	0.09988	0.00102	0.04600	0.05096	0.04600		0.1999
CO-24	17	67.0	0.572	0.09988	0.00102	0.04600	0.05096	0.04600		0.1999
CO-25	9	30.3	0.820	0.09988	0.00102	0.04600	0.05096	0.04600		0.1999
CO-26	9	29.8	0.820	0.09988	0.00102	0.04600	0.05096	0.04600		0.1999
CO-27	8	29.5	0.806	0.09988	0.00102	0.04600	0.05096	0.04600		0.1999
CO-28	8	29.0	0.802	0.09952	0.00106	0.04070	0.05080	0.04070		0.1942
CO-30	11	30.0	0.573	0.09971	0.00105	0.04600	0.05091	0.04600		0.1998
CO-31	16	30.0	0.810	0.09655	0.00104	0.09700	0	0.19560		0.1966
CO-36	16	30.0	0.809	0.09873	0.00103	0.09700	0	0	0.19910*	0.1995
CO-37	16	30.0	0.810	0.09946	0.00105	0.03200	0.06678	0		0.2014
CO-40	18	29.8	0.817	0.09959	0.00103	0.09700	0	0	0.19870°	0.1997
CO-41	7	30.8	0.809	0.09900	0.00106	0.04600	0.05056	0.04600		0.1987
CO-43	18	30.0	0.807	0.09977	0.00102	0.09700	0	0	0.19100+	0.1959
CO-47	7	29.8	0.810	0.09945	0.00105	0.04600	0.05078	0.04600		0.1994
Base	@	29.7	0.810	0.09948	0.00105	0.04600	0.05079	0.04600		0.1994
CO-42		29.0	0	0.09914	0.00104	0.04600	0.05061	0.04600		0.1989

* Nitrate Ion.
o Chloride Ion.
\+ Bromide Ion.
@ Figures 8, 9, 11, 13, 17 and 18.

Table XI

Tabulation of Cupric Ion Concentration

for Chalcocite Dissolution Experiments

Experiment Number	Elapsed Time (Min)	Experimental Cupric Ion Concentration (M/L)	Adjusted Cupric Ion Concentration (M/L)
CO-16	0.0	0.001030	0.000999
	30.0	0.001599	0.001253
	60.0	0.001932	0.001586
	120.0	0.002392	0.002047
	240.0	0.003280	0.002934
	300.0	0.003726	0.003380
	360.0	0.004061	0.003716
	420.0	0.004403	0.004057
	480.0	0.004737	0.004391
	540.0	0.004994	0.004648
	600.0	0.005268	0.004922
CO-17	0.0	0.001029	0.000999
	30.0	0.001554	0.001209
	60.0	0.001799	0.001454
	120.0	0.002128	0.001783
	180.0	0.002451	0.002106
	240.0	0.002753	0.002408
	300.0	0.003007	0.002662
	360.0	0.003289	0.002944
	420.0	0.003571	0.003226
	480.0	0.003845	0.003500
	540.0	0.004140	0.003795
	600.0	0.004377	0.004032
CO-18	0.0	0.001012	0.000999
	30.0	0.001455	0.001128
	60.0	0.001645	0.001318
	120.0	0.001850	0.001523
	180.0	0.002011	0.001683
	240.0	0.002152	0.001824
	300.0	0.002332	0.002005
	360.0	0.002530	0.002203
	420.0	0.002610	0.002282
	480.0	0.002784	0.002456
	540.0	0.002994	0.002667
	600.0	0.003043	0.002716

Table XI

Continued

Experiment Number	Elapsed Time (Min)	Experimental Cupric Ion Concentration (M/L)	Adjusted Cupric Ion Concentration (M/L)
CO-19	0.0	0.001022	0.000999
	30.0	0.001625	0.001287
	60.0	0.001832	0.001494
	120.0	0.002174	0.001836
	180.0	0.002495	0.002157
	240.0	0.002794	0.002456
	300.0	0.003128	0.002790
	360.0	0.003359	0.003021
	420.0	0.003752	0.003414
	480.0	0.003996	0.003658
	540.0	0.004240	0.003902
	600.0	0.004518	0.004180
CO-20	0.0	0.001040	0.000999
	30.0	0.001592	0.001237
	60.0	0.001759	0.001404
	120.0	0.002115	0.001760
	180.0	0.002440	0.002085
	240.0	0.002795	0.002440
	300.0	0.003063	0.002709
	360.0	0.003362	0.003007
	420.0	0.003616	0.003261
	480.0	0.003883	0.003528
	540.0	0.004092	0.003737
	600.0	0.004351	0.003996
CO-23	0.0	0.001022	0.000999
	30.0	0.001776	0.001438
	66.0	0.002272	0.001935
	120.0	0.002779	0.002441
	180.0	0.003470	0.003132
	240.0	0.003916	0.003579
	300.0	0.004407	0.004069
	360.0	0.004853	0.004516
	420.0	0.005310	0.004973
	480.0	0.005741	0.005404
	540.0	0.005927	0.005589
	600.0	0.006277	0.005939

Table XI

Continued

Experiment Number	Elapsed Time (Min)	Experimental Cupric Ion Concentration (M/L)	Adjusted Cupric Ion Concentration (M/L)
CO-24	0.0	0.001031	0.000999
	30.0	0.002008	0.001662
	60.0	0.002488	0.002142
	120.0	0.003301	0.002955
	180.0	0.003981	0.003635
	240.0	0.004540	0.004194
	300.0	0.005149	0.004803
	360.0	0.005563	0.005217
	420.0	0.005937	0.005591
	480.0	0.006279	0.005933
	540.0	0.006665	0.006318
	610.0	0.007171	0.006824
CO-25	0.0	0.001070	0.000999
	32.0	0.002278	0.001893
	60.0	0.002650	0.002265
	120.0	0.003386	0.003001
	180.0	0.004105	0.003720
	240.0	0.004792	0.004407
	300.0	0.005222	0.004837
	360.0	0.006018	0.005633
	420.0	0.006714	0.006329
	480.0	0.007421	0.007036
	540.0	0.007942	0.007557
CO-26	0.0	0.001030	0.000999
	30.0	0.001357	0.001011
	60.0	0.001459	0.001113
	120.0	0.001701	0.001355
	181.0	0.001853	0.001507
	241.0	0.002048	0.001702
	300.0	0.002174	0.001829
	360.0	0.002320	0.001975
	420.0	0.002519	0.002173
	480.0	0.002730	0.002384
	544.0	0.002980	0.002634
	600.0	0.003021	0.002676

Table XI

Continued

Experiment Number	Elapsed Time (Min)	Experimental Cupric Ion Concentration (M/L)	Adjusted Cupric Ion Concentration (M/L)
CO-27	0.0	0.001059	0.000999
	30.0	0.001749	0.001374
	60.0	0.001918	0.001543
	120.0	0.002304	0.001929
	180.0	0.002650	0.002276
	240.0	0.002948	0.002573
	300.0	0.003318	0.002944
	360.0	0.003571	0.003196
	420.0	0.003917	0.003542
	480.0	0.004194	0.003820
	540.0	0.004446	0.004071
	600.0	0.004748	0.004374
CO-28	0.0	0.001059	0.000999
	30.0	0.001566	0.001192
	60.0	0.001714	0.001340
	120.0	0.001930	0.001556
	180.0	0.002092	0.001718
	240.0	0.002238	0.001864
	300.0	0.002393	0.002019
	360.0	0.002562	0.002187
	420.0	0.002696	0.002322
	540.0	0.002998	0.002624
	600.0	0.003193	0.002819
CO-30	0.0	0.001046	0.000999
	30.0	0.001578	0.001217
	60.0	0.001732	0.001371
	120.0	0.001995	0.001633
	180.0	0.002197	0.001835
	240.0	0.002489	0.002127
	300.0	0.002697	0.002336
	420.0	0.003162	0.002800
	480.0	0.003384	0.003022
	540.0	0.003606	0.003244
	600.0	0.003815	0.003453

Table XI

Continued

Experiment Number	Elapsed Time (Min)	Experimental Cupric Ion Concentration (M/L)	Adjusted Cupric Ion Concentration (M/L)
CO-31	0.0	0.001037	0.000999
	30.0	0.001734	0.001381
	60.0	0.002033	0.001680
	120.0	0.002574	0.002221
	180.0	0.003014	0.002662
CO-36	0.0	0.001029	0.000999
	34.0	0.001760	0.001415
	60.0	0.001975	0.001630
	120.0	0.002458	0.002113
	181.0	0.002922	0.002577
	240.0	0.003335	0.002991
	300.0	0.003755	0.003411
	360.0	0.004169	0.003825
	420.0	0.004533	0.004188
	480.0	0.004878	0.004533
	540.0	0.005185	0.004840
	600.0	0.005505	0.005160
CO-37	0.0	0.001052	0.000999
	29.0	0.001718	0.001350
	60.0	0.001936	0.001569
	120.0	0.002289	0.001922
	180.0	0.002575	0.002207
	240.0	0.002924	0.002556
	300.0	0.003220	0.002852
	362.0	0.003501	0.003133
	423.0	0.003827	0.003460
	480.0	0.004085	0.003718
	540.0	0.004359	0.003991
	600.0	0.004586	0.004218

Table XI

Continued

Experiment Number	Elapsed Time (Min)	Experimental Cupric Ion Concentration (M/L)	Adjusted Cupric Ion Concentration (M/L)
CO-40	0.0	0.001032	0.000999
	30.0	0.004103	0.003756
	60.0	0.006065	0.005717
	120.0	0.010340	0.009993
	180.0	0.015276	0.014929
	240.0	0.018087	0.017740
	300.0	0.020769	0.020422
	360.0	0.023903	0.023556
	420.0	0.026825	0.026477
	540.0	0.032489	0.032142
	600.0	0.034488	0.034141
CO-41	0.0	0.001064	0.000999
	30.0	0.001735	0.001356
	60.0	0.001920	0.001541
	120.0	0.002286	0.001907
	180.0	0.002658	0.002279
	240.0	0.003008	0.002629
	300.0	0.003291	0.002912
	360.0	0.003591	0.003211
	420.0	0.003957	0.003577
	480.0	0.004190	0.003810
	540.0	0.004456	0.004077
	600.0	0.004789	0.004410
CO-42	0.0	0.001044	0.000999
	30.0	0.001511	0.001151
	60.0	0.001566	0.001206
	120.0	0.001570	0.001210
	180.0	0.001612	0.001252
	240.0	0.001624	0.001264
	300.0	0.001666	0.001306
	474.0	0.001645	0.001285
	600.0	0.001620	0.001260

Table XI

Continued

Experiment Number	Elapsed Time (Min)	Experimental Cupric Ion Concentration (M/L)	Adjusted Cupric Ion Concentration (M/L)
CO-43	0.0	0.001017	0.000999
	30.0	0.005951	0.005619
	60.0	0.011884	0.011552
	120.0	0.021406	0.021074
	180.0	0.029353	0.029021
	243.0	0.036881	0.036549
	300.0	0.039728	0.039396
	360.0	0.042416	0.042084
	480.0	0.043840	0.043508
	540.0	0.044789	0.044457
	600.0	0.046686	0.046355
CO-47	0.0	0.001047	0.000999
	30.0	0.001661	0.001299
	60.0	0.001819	0.001457
	120.0	0.002198	0.001836
	240.0	0.002838	0.002476
	300.0	0.003234	0.002872
	360.0	0.003428	0.003065
	420.0	0.003773	0.003411
	480.0	0.004058	0.003696
	540.0	0.004363	0.004001
	600.0	0.004663	0.004300
CO-BS	0.0	0.001050	0.000999
	30.0	0.001654	0.001289
	60.0	0.001876	0.001511
	120.0	0.002201	0.001836
	240.0	0.002846	0.002481
	300.0	0.003173	0.002808
	360.0	0.003431	0.003066
	420.0	0.003762	0.003397
	480.0	0.004025	0.003660
	540.0	0.004314	0.003949
	600.0	0.004603	0.004238

Table XII

Experimental and ASTM X-ray Powder Diffraction Data for Unleached Chalcocite.

Cu_2S hkl Reflection	Cu_2S ASTM* d Spacing	Experimental d Spacing	SiO_2 ASTM° d Spacing	Experimental I/I_1
080	3.41			
		3.35	3.34	100
233,153	3.33	3.33		23
322	3.31			
024	3.27	3.27		12
		3.21@		12
262	3.18	3.19		24
351	3.12			
342	3.05	3.06		14
280,400	2.96	2.96		24
182	2.95			
204,144	2.93			
411	2.88	2.89		8
173,224	2.86	2.88		9
333	2.82	2.83		4
431	2.76	2.77		12
362	2.73	2.73		36
440	2.72			
244	2.69	2.70		8
422	2.67	2.67		15
291,164	2.64			
115,353	2.62	2.63		9
451	2.56	2.57		9
0.10.2	2.53	2.53		24
442,135	2.52	2.52		49

Table XII

Continued

Cu_2S hkl Reflection	Cu_2S ASTM* d Spacing	Experimental d Spacing	SiO_2 ASTM° d Spacing	Experimental I/I_1
1.10.2	2.48	2.48		31
413,193	2.47	2.47		34
		2.46	2.46	22
215	2.44			
344	2.40	2.41		54
084	2.40			
433	2.39			
373,235+	2.37			
471,2.10.2	2.33	2.33		27
		2.29#		6
		2.28	2.28	6
480,502+	2.24	2.25		32
		2.24	2.24	12
404	2.23			
315,075+	2.22	2.22		15
522,106	2.21			
126	2.18			
1.11.3,046	2.14			
		2.13	2.13	19
444	2.12			
		2.10#		6
533	2.04			
2.12.2	2.03	2.03		6
562,246	2.01	2.01		13
464	2.00			
415	1.99			
600	1.98	1.98	1.98	69
3.12.0	1.97			
553	1.96	1.96		24
580,435+	1.95			

Table XII

Continued

Cu_2S hkl Reflection	Cu_2S ASTM* d Spacing	Experimental d Spacing	SiO_2 ASTM° d Spacing	Experimental I/I_1
631,493	1.92			10
266	1.91	1.91		
3.12.2,117	1.90	1.90		10
346,086	1.88	1.88		59
137	1.86			
651	1.84			
		1.82	1.82	12
366,237+	1.80	1.80	1.80	12
2.14.2,564	1.79			
633,475+	1.78			
		1.71		22
		1.70 @		18
		1.69 #		13
			1.67	
		1.66	1.66	12
		1.64		9
		1.54	1.54	12

* ASTM Powder Diffraction Card No. 12-227 and 12-227a
o ASTM Powder Diffraction File Card No. 5-9490
@ ASTM Powder Diffraction File Card No. 9-328 for Cu_2S
\# ASTM Powder Diffraction File Card No. 12-1205 for $Cu_{1.96}S$

Table XIII

Experimental and ASTM X-ray Powder Diffraction Data for Leached Chalcocite.

Cu_2S hkl Reflection	Cu_2S ASTM* d Spacing	Experimental d Spacing	CuS ASTM° d Spacing	CuS hkl Reflection	SiO_2 ASTM+ d Spacing	Experimental I/I_1
080	3.41					
		3.35			3.34	100
233,153	3.33					
322	3.31		3.29	100		
024	3.27	3.27				14
		3.23	3.22 ⑥	101		22
262	3.18					
351	3.12					
342	3.05	3.06	3.05 ⑤	102		53
280,400	2.96					
182	2.95					
204,144	2.93					
411	2.88					
173,224	2.86					
333	2.82					
		2.80	2.81 ④	103		
431	2.76					
362	2.73					
440	2.72		2.72	006		
244	2.69	2.70				28
422	2.67					
291,164	2.64					
115,353	2.62					
451	2.56					
0.10.2	2.53					
442,135	2.52	2.52				12
1.10.2	2.48					

Table XIII

Continued

Cu_2S hkl Reflection	Cu_2S ASTM* d Spacing	Experimental d Spacing	CuS ASTM° d Spacing	CuS hkl Reflection	SiO_2 ASTM+ d Spacing	Experimental I/I_1
413,193	2.47					
		2.46			2.46	14
215	2.44					
344	2.40					
084	2.40					
433	2.39					
373,235+	2.37					
471,2.10.2	2.33					
			2.32	105		
		2.28			2.28	13
480,502+	2.24	2.24				10
404	2.23					
315,075+	2.22					
522,106	2.21					
126	2.18					
1.11.3,046	2.14					
		2.13			2.13	5
444	2.12					
			2.10	106		
533	2.04		2.04	008		
2.12.2	2.03					
562,246	2.01					
464	2.00					
415	1.99					
600	1.98	1.98			1.98	8
3.12.0	1.97					
553	1.96					
580,435+	1.95					

Table XIII

Continued

Cu_2S hkl Reflection	Cu_2S ASTM* d Spacing	Experimental d Spacing	CuS ASTM° d Spacing	CuS hkl Reflection	SiO_2 ASTM+ d Spacing	Experimental I/I_1
631,493	1.92					
266	1.91					
			1.90	110		
3.12.2,117	1.90	1.89	1.90 ③	107		92
346,086	1.88					
137	1.86					
651	1.84	1.84				9
		1.82			1.82	21
366,237+	1.80				1.80	
2.14.2,564	1.79		1.74	108		
		1.70 @				7
					1.67	
					1.66	
			1.63	201		
		1.61	1.61 ②	202		8
		1.57	1.57 ①	203		20
			1.56	116		
		1.54			1.54	10

* ASTM Powder Diffraction Card No. 12-227 and 12-227a
o ASTM Powder Diffraction Card No. 6-0464
\+ ASTM Powder Diffraction Card No. 5-0490
@ ASTM Powder Diffraction Card No. 9-328 for Cu_2S

Appendix B. Methods of Data Analysis

Measurement and Correction of System Pressure

System pressure was measured with a mercury or water manometer and compared with barometric pressure to obtain the absolute pressure. A mercury barometer was used to obtain the barometric pressure.

The mercury barometer readings were reduced to a temperature of $0^{o}C$ using equation (68) where CBP = corrected

$$CBP = BP - 0.104 \times T \qquad (68)$$

barometric pressure, BP = experimental barometric pressure and T = the temperature of the barometer. The mercury manometer pressure was found from equation (69) where

$$MP = RH - LH \qquad (69)$$

MP = pressure indicated by mercury manometer, RH = height of mercury in the right arm of the manometer and RL = height of mercury in the left arm of the manometer. The mercury manometer pressure was reduced to $0^{o}C$ using equation (70) where CMP = corrected mercury pressure, L_o = length

$$CMP = MP - L_o(\alpha T + \beta T^2) \qquad (70)$$

of the mercury column at $0^{o}C$, α and β = coefficients of cubical expansion for mercury and T = temperature of the manometer.

The water manometer pressure, WP, was found using equation (71) where RHW and LHW are the heights of the

$$WP = RHW - LHW \tag{71}$$

right and left arms of the water manometer. The water manometer pressure was reduced to 15.5°C and converted to mm Hg using equation (72) where CWP = corrected water

$$CWP = \frac{WP - H_o(1.00000/D - 1.00075)}{13.62} \tag{72}$$

manometer pressure, H_o = height of the water column at 15.5°C and D = density of water at the temperature of the manometer. D was determed using equation (73) where

$$D = 1.00010 + 0.00001\ T - 0.0000052\ T^2 \tag{73}$$

T = temperature of the manometer.

The absolute system pressure was found by equation (74) where SP = system pressure. CMP may be replaced by

$$SP = CBP + CMP \tag{74}$$

CWP when a water manometer was used.

Calculation of Oxygen Consumption

The moles of oxygen consumed was found using equation (75) where O_2 = moles of oxygen consumed, SP_o = initial

$$O_2 = \frac{(SP_o - SP_f)\ V}{(760.0)(82.06)\ T} \tag{75}$$

pressure, SP_f = final pressure, V = gas volume of the system and T = the experimental temperature. Equation (75) is based on the ideal gas law.

Determination and Adjustment of Cu^{+2} Ion Concentration

Cupric ion concentration was determined by atomic absorption spectroscopy. Each concentration value was corrected for the difference in experimental temperature and the calibration temperature of the glassware, solution volume change due to sampling and evaporation, variation in initial solution volume and non-oxidative solubility of chalcocite.

A least squares line was fitted to atomic absorption readout vs. ppm for a set of copper standards (5, 10, 15, and 20 ppm). The concentration of unknown samples in ppm was calculated from the atomic absorption readout of the unknown and the least squares line equation. The concentration was then multiplied by the dilution factor to determine the original Cu^{+2} ion concentration of the sample. The dilution factor was corrected for temperature difference between the sample and the calibration temperature of the glassware. The corrected dilution factor is given by equation (76) where F = original dilution factor, CF =

$$CF = F(0.99823)/D \qquad (76)$$

corrected dilution factor and D = density of water at the experimental temperature.

Each time a sample was removed from the system, the solution volume was reduced and an error was introduced into the calculation of Cu^{+2} ion concentration. Consequently,

each concentration value was corrected for the change in solution volume by converting all concentrations to a total constant volume of 2.5 l. Thus, all concentrations are strictly comparable for each sample and each experiment. In addition, this correction removed the effect of small variations in the initial volume of the solution.

The natural, non-oxidative solubility of chalcocite was subtracted from each concentration value. All concentration values were then converted from ppm to moles/liter.

Polynomial Curve Fitting

A polynomial curve of the form given by equation (77) was fitted to experimental oxygen partial pressure vs.

$$Y = A_1 + A_2X + A_3X^2 \qquad (77)$$

time and Cu^{+2} ion concentration vs. time data using the least squares technique given by Worthing and Geffner (1943).

Data Analysis

All of the data analysis and tabulation discussed in this appendix was carried out with the aid of an IBM 360 digital computer.

Appendix C. Analytic Procedures

Analytic Procedures

Cupric ion in leach solutions was determined by atomic absorption spectroscopy. Each sample was diluted to the concentration range 5 to 20 ppm immediately after it was taken from the leaching system. The dilution of each sample was made in one step to eliminate as much volumetric error as possible. 1 N HCl was added to each dilution to keep the pH of the diluted sample below a value of 1.

Hydrogen ion concentration was determined by NaOH titration. The NaOH solutions were standardized against potassium hydrogen phthalate. The end point of unknown titrations was set at a pH value of 4 and was determined with a pH meter. The low endpoint pH was selected to prevent the hydrolysis of cupric ion. Since the change in hydrogen ion concentration was the important quantity being sought, no error was introduced by selecting pH 4 as an endpoint.

Sulfate ion concentration was determined by the standard, $BaSO_4$, gravimetric method given by Olson, Koch and Pimentel (1956). Oxidation of sulfur species to sulfate was accomplished by adding saturated bromine water to the hot solution. The excess bromine was boiled off prior to $BaSO_4$ precipitation.

This thesis is accepted on behalf of the faculty of the Institute by the following committee:

Date May 21, 1970